CrossMark

J. Fluid Mech. (2015), *vol.* 773, *pp.* 1–33. © Cambridge University Press 2015
doi:10.1017/jfm.2015.242

The Taylor–Melcher leaky dielectric model as a macroscale electrokinetic description

Ory Schnitzer[1,†] **and Ehud Yariv**[1]

[1]Department of Mathematics, Technion - Israel Institute of Technology, Haifa 32000, Israel

(Received 26 August 2014; revised 26 January 2015; accepted 21 April 2015;
first published online 14 May 2015)

While the Taylor–Melcher electrohydrodynamic model entails ionic charge carriers, it addresses neither ionic transport within the liquids nor the formation of diffuse space-charge layers about their common interface. Moreover, as this model is hinged upon the presence of non-zero interfacial-charge density, it appears to be in contradiction with the aggregate electro-neutrality implied by ionic screening. Following a brief synopsis published by Baygents & Saville (*Third International Colloquium on Drops and Bubbles*, AIP Conference Proceedings, vol. 7, 1989, American Institute of Physics, pp. 7–17) we systematically derive here the macroscale description appropriate for leaky dielectric liquids, starting from the primitive electrokinetic equations and addressing the double limit of thin space-charge layers and strong fields. This derivation is accomplished through the use of matched asymptotic expansions between the narrow space-charge layers adjacent to the interface and the electro-neutral bulk domains, which are homogenized by the strong ionic advection. Electrokinetic transport within the electrical 'triple layer' comprising the genuine interface and the adjacent space-charge layers is embodied in effective boundary conditions; these conditions, together with the simplified transport within the bulk domains, constitute the requisite macroscale description. This description essentially coincides with the familiar equations of Melcher & Taylor (*Annu. Rev. Fluid Mech.*, vol. 1, 1969, pp. 111–146). A key quantity in our macroscale description is the 'apparent' surface-charge density, provided by the transversely integrated triple-layer microscale charge. At leading order, this density vanishes due to the expected Debye-layer screening; its asymptotic correction provides the 'interfacial' surface-charge density appearing in the Taylor–Melcher model. Our unified electrohydrodynamic treatment provides a reinterpretation of both the Taylor–Melcher conductivity-ratio parameter and the electrical Reynolds number. The latter, expressed in terms of fundamental electrokinetic properties, becomes $O(1)$ only for intense applied fields, comparable with the transverse field within the space-charge layers; at this limit the asymptotic scheme collapses. Surface-charge advection is accordingly absent in the macroscale description. Owing to the inevitable presence of (screened) net charge on the genuine interface, the drop also undergoes electrophoretic motion. The associated flow, however, is asymptotically smaller than that corresponding to the Taylor–Melcher circulation. Our successful matching procedure contrasts the analysis

† Present address: Department of Mathematics, Imperial College London, South Kensington Campus, London SW7 2AZ, UK. Email address for correspondence: udi@technion.ac.il

https://doi.org/10.1017/jfm.2015.242 Published online by Cambridge University Press

of Baygents & Saville, who considered more general electrolytes and were unable to directly match the inner and outer regions. We discuss this difference in detail.

Key words: drops and bubbles, electrohydrodynamic effects

1. Introduction

The Taylor–Melcher leaky dielectric model describes electrohydrodynamic phenomena in poorly conducting liquids. In this model, volumetric charge is completely absent. The liquids are described as dielectric materials that nonetheless possess finite Ohmic conductivities; this description reflects Taylor's (1966) realization that, however small their conductivity is, poorly conducting liquids are fundamentally different from perfect dielectrics. Specifically, rather then satisfying the interfacial condition of electric-displacement continuity, pertinent to dielectric liquids, the electric-field distribution is set at steady state by the condition of electric-current continuity. With the inevitable jump in the electric displacement, the field distribution satisfying the latter condition is generally accompanied by a non-zero surface-charge distribution at the interface. The electrical shear forces acting on the charged interface then give rise to fluid motion.

The model put forward by Taylor (1966) in the context of electrohydrodynamic drop deformation was revisited by Melcher & Taylor (1969), and has since been the basis for numerous investigations in electrohydrodynamic phenomena (Feng & Scott 1996; Feng 1999; Craster & Matar 2005; Salipante & Vlahovska 2014). The interfacial current-continuity condition was generalized to account for surface convection of charge, whose relative magnitude is quantified by the electric Reynolds number. Taylor's analysis, where surface convection is neglected, thus corresponds to low values of this dimensionless group. In this limit, and for a specified interface geometry, the electrostatic problem is decoupled from the flow, satisfying a linear problem. This allows for straightforward analytic solutions.

The charge carriers in the leaky dielectric model are accounted for only through the prescription of (uniform) liquid conductivities. Thus, the Taylor–Melcher scheme avoids the need to account for ionic transport, a nonlinear mechanism underlying electrokinetic phenomena (Saville 1977). Analysis of leaky dielectric and electrokinetic flows have therefore evolved more-or-less independently, with the two scientific communities being essentially foreign.

Since the charge carriers in leaky dielectric liquids are typically ions (Saville 1997), a troubling question arises. It is well known that the presence of charged interfaces in an ion-carrying liquid results in the formation of adjacent diffuse ('Debye') layers, within the liquid, of charge opposite to that on the interface. Since the Taylor–Melcher model does not allow for volumetric charges, these two layers are absent in it. Moreover, it is not *a priori* evident whether the surface-charge density appearing in the Taylor–Melcher model may be viewed as a coarse-grained aggregate quantity, namely the 'apparent' charge of the combined triple-layer system: after all, one might actually expect that this apparent charge would vanish by screening.

This paradox, along with additional ambiguities in the Taylor–Melcher model, emphasizes the need for a unified electrohydrodynamic approach, starting from the fundamental electrokinetic description. Our goal is to address this challenge in the context of Taylor's classical problem: a spherical drop in a uniform field. To account

https://doi.org/10.1017/jfm.2015.242 Published online by Cambridge University Press

for the passage of current through the drop interface, as postulated by Taylor, the physicochemical model of the interface must allow for sorption of the charge carriers, here being simply the salt ions. By applying an asymptotic limit which properly represents 'leaky dielectric liquids,' a systematic analysis would reveal whether the Taylor–Melcher model indeed emerges.

Since leaky dielectric liquids are poor conductors, their microscale description typically involves small ionic concentrations. Saville (1997) provides the characteristic value 10^{-7} m for the corresponding Debye thickness (see (4.7)). In electrokinetic phenomena involving colloidal particles, this estimate is easily comparable with particle size; when considering drops, however, which can reach millimetres in size, this estimate actually suggests considering the limit where the ratio δ of Debye thickness to drop size is exceedingly small. This asymptotic limit has been extensively studied in the context of electrokinetic phenomena involving solid particles (Morrison 1970; Derjaguin & Dukhin 1974; O'Brien 1983; Anderson 1989; Schnitzer & Yariv 2012*a*), ion-selective granules (Ben, Demekhin & Chang 2004; Yariv 2010), metal drops (Ohshima, Healy & White 1984; Schnitzer, Frankel & Yariv 2013) and gas bubbles (Schnitzer, Frankel & Yariv 2014).

Another fundamental parameter appearing in the electrokinetic problem is the ratio β of the drop-scale voltage associated with the applied field and the thermal voltage ($\approx$25 mV), see (4.35). For electrokinetic phenomena about small colloidal particles, Saville (1977) provides the typical value 5×10^{-4} for β. This estimate assumes a particle of radius 0.1 μm in a field of magnitude 10 V cm^{-1}; electrokinetic effects are observed also with slightly larger particles and stronger fields allowing for $\beta = O(1)$. Much larger β values are found for drops in leaky dielectric fluids. These large values of the dimensionless field are not only due to the large length scales, but also due to the strong fields which are typically applied. Thus, Saville (1997) provides the typical figure 10^3 corresponding to a drop of millimetric size exposed to an electric field of magnitude 10^3 V cm^{-1}. The limit $\delta \ll 1$ must therefore be accompanied by the limit $\beta \gg 1$.

The above twofold limit was first employed in a short synopsis by Baygents & Saville (1989). Specifically, Baygents & Saville (1989) considered the limit

$$1 \ll \beta \ll 1/\delta, \tag{1.1}$$

and applied it to a relatively standard electrokinetic model, where the microscale transport of ions through the interface is modelled through simple sorption kinetics. (For the above-mentioned scenario of a millimetric drop in a strong electric field, (1.1) requires a Debye length $\ll \mu$m.) The fluid domain was asymptotically decomposed into 'inner' diffuse-charge layers, of $O(\delta)$ thickness, and 'outer' bulk regions, which are homogenized by the intense ionic advection. Baygents & Saville (1989) were unable to directly match the inner and outer regions, and suggested that a separate analysis of an intermediate layer, of thickness $1/\beta$, is required. The resulting matching procedure, however, is not provided in that concise synopsis, nor is the consequent macroscale description. Baygents & Saville (1989) do provide the eventual flow field, which is the same as that calculated by Taylor (1966).

In the present paper we revisit the Baygents–Saville approach. We employ the same microscale electrokinetic model used by Baygents & Saville (1989), which for the purpose of brevity and clarity is here limited to binary electrolytes. In this case, we do manage to match the inner and outer regions, and thereby obtain a macroscale 'coarse-grained' description, where the Debye-layer physics appear

https://doi.org/10.1017/jfm.2015.242 Published online by Cambridge University Press

as effective boundary conditions. This description closely resembles the equations outlined by Melcher & Taylor (1969), but with several important differences. These include the absence of charge convection, the re-interpretation of the conductivity-ratio parameter of Taylor (1966), and the appearance of electrophoretic drop motion at a higher asymptotic order.

Our paper is constructed as follows. Following a physical description of the problem in § 2, we provide in § 3 intuitive arguments, describing how coarse graining an electrokinetic model can give rise to a leaky-dielectric-type model. We then shift to a systematic treatment of the problem, formulating in § 4 a microscale problem using the *ab initio* electrokinetic description, following Baygents & Saville (1989). In § 5 we apply the Baygents–Saville limit (1.1), and derive the outer-bulk description. The diffuse-charge layers are described and analysed at leading order in § 6. The analysis of the subsequent asymptotic order is carried out in § 7, where an asymptotic matching procedure provides the requisite effective boundary conditions. The resulting macroscale model is recapitulated in § 8 using the familiar leaky dielectric scaling. In § 9 we discuss the surprising differences between our analysis and those in the synopsis of Baygents & Saville (1989). We conclude in § 10, discussing at length the unique features of the macroscale description we obtain, and in particular the differences with the Taylor–Melcher model.

To the best of the authors' knowledge, the work of Baygents & Saville (1989) is the only attempt to derive the equivalent of the Taylor–Melcher model from the more primitive electrokinetic description using the limit process appropriate for describing leaky dielectric liquids. Our analysis, which succeeds in deriving such a macroscale model, contributes toward a unified view of interfacial electrohydrodynamics.

2. Physical problem

We consider essentially the same physicochemical problem as Baygents & Saville (1989), motivated by the prototypic problem addressed by Taylor (1966). An immiscible liquid drop of radius a_* (dimensional quantities are decorated hereafter with an asterisk) is suspended in another liquid. The viscosity and dielectric permittivity of the suspending liquid are respectively denoted by μ_* and ϵ_*; consistently with the original notation of Taylor (1966), the viscosity and dielectric permittivity of the suspended drop are respectively denoted by μ_*/M and ϵ_*/S. For simplicity we consider symmetric electrolytes with ionic valencies $\pm z$; the two ionic species then possess an identical equilibrium concentration (say $\mathscr{C}_*$) at large distances away from the drop. The ionic diffusivites of cations and anions within the suspending liquid are respectively denoted by $D_*^{\pm}$; in view of the Einstein–Smoluchowski relation, the respective diffusivities within the drop are $MD_*^{\pm}$. As in Baygents & Saville (1989), passage of current through the interface is made possible by assuming that the ions undergo sorption there. Specifically, we employ the simplest possible model of fast reactions, where the excess-surface concentration is proportional to that in the solution.

A uniform and constant electric field of magnitude $\mathscr{E}_*$ is externally applied. Our interest is in the steady-state flow which is reached in a reference frame comoving with the drop. As in Taylor (1966), we assume that capillary forces are strong enough such that the drop remains approximately spherical.

The only difference between the preceding problem and that considered by Baygents & Saville (1989) is the limitation to a binary electrolyte.

https://doi.org/10.1017/jfm.2015.242 Published online by Cambridge University Press

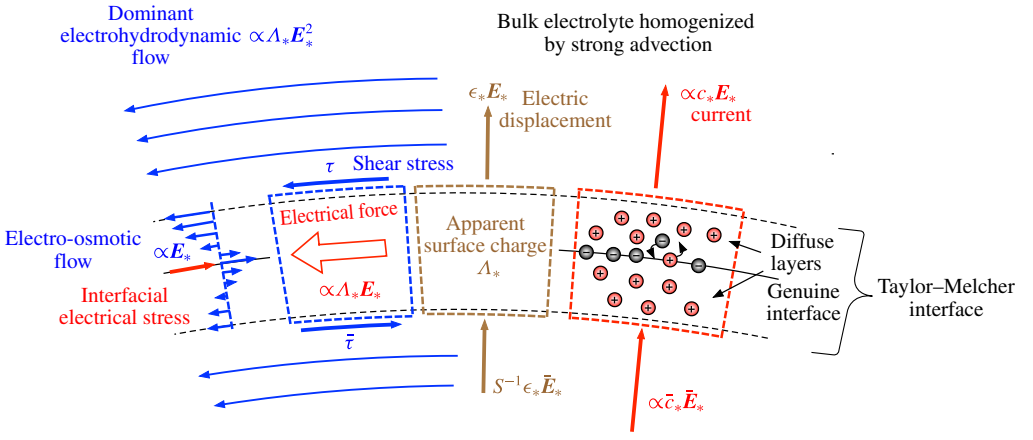


FIGURE 1. (Colour online) Schematic accompanying the intuitive overview of § 3. Description from right to left. (i) Asymmetric ionic sorption implies an 'equilibrium' interfacial charge, screened by two adjacent diffuse layers. Sorption also allows electric currents associated with the applied field to pass through the compound Taylor–Melcher interface, while resulting in only a slight perturbation to the triple-layer structure. (ii) Gauss law on the depicted control volume reveals that the perturbed triple layer deviates from electro-neutrality. The overall, or apparent, charge per unit area is Λ_*. (iii) The tangential field is approximately uniform on the Debye scale. Its action on the apparent charge, itself induced by the field, results in a macroscopic stress jump which drives the dominant flow field. (iv) The action of the field on the equilibrium charge distribution results in steep electro-osmotic flow profiles. While this flow, and the macroscopic slip it entails, is relatively weak, the viscous shear inflicted on the microscopic interface is strong. It is exactly balanced by the interfacial electric stress associated with the equilibrium surface-excess ion concentration.

3. Intuitive overview

It is useful to precede the detailed asymptotic treatment provided in the following sections with an intuitive outline of some of the main results (figure 1). In what follows, we employ heuristic assumptions and gross approximations; all of these are clarified and substantiated in the systematic analysis appearing in the following sections.

As explained in § 2, we assume sorption kinetics in the physicochemical model of the interface, so as to allow for the passage of current. An inevitable consequence of that model is the existence of interfacial charge, even in the absence of an applied field. This 'equilibrium' charge is screened by two diffuse-charge layers on both sides of the interface. Their characteristic thickness $1/\kappa_*$ is assumed thin compared with drop size a_*. Following standard electrokinetic descriptions in the thin-double-layer limit (Schnitzer & Yariv 2012*a*) it is expected that the ions in the two diffuse layers are Boltzmann distributed with the electric potential satisfying the one-dimensional Poisson–Boltzmann equations; this triple-layer structure trivially generalizes the familiar Gouy–Chapman structure of the electrical double layer. Using traditional notation we denote the potential difference, at equilibrium, between the interface and the outer edges of the external and internal diffuse-charge layers by ζ_* and $\bar{\zeta}_*$, respectively. These are of the order of the thermal voltage $\varphi_* = k_* T_*/ze_*$ (k^*T^* being the Boltzmann temperature and e^* the elementary charge). We consider

https://doi.org/10.1017/jfm.2015.242 Published online by Cambridge University Press

the limit where the applied field is large compared with thermal scale φ_*/a_* but is nonetheless small compared with the transverse field in the narrow Debye layers, which is of order $\kappa_*\varphi_*$:

$$\frac{\varphi_*}{a_*} \ll \mathscr{E}_* \ll \kappa_*\varphi_*. \tag{3.1}$$

This is the dimensional version of the Baygents–Saville limit (1.1).

We start with the effect of the applied field on the bulk liquid domains lying outside the two diffuse-charge layers. These domains are approximately electro-neutral, with the cation and anion concentrations being nearly identical. The ionic concentration is uniform far away from the drop. In principle, concentration polarization on the drop scale may by triggered by effective 'surface' currents which originate at the Debye-scale transport. The extent and topology of such concentration non-uniformities are determined by a balance between advection by the field-induced flow, characterized by the velocity scale $\mathscr{U}_*$, and Brownian diffusion. With the applied field assumed strong, it is plausible that the flow is strong as well, in the sense that the Péclet number $Pe = a_*\mathscr{U}_*/D_*$ is large, D_* being a characteristic ionic diffusivity. Thus, the ionic concentration is dominated by advection, and possesses uniform values in the external and internal bulk domains. The concentration value in the suspending liquid is simply given by the far-field concentration, namely c^*; the drop concentration, say $\bar{c}_*$, is generally different. Thus, bulk concentration polarization effects, often important in electrokinetic analyses (Chu & Bazant 2006; Mani & Bazant 2011; Schnitzer *et al.* 2013), are here prevented by the dominance of advection. The concentration deviations triggered by Debye-scale fluxes are confined to thin diffusive layers where the concentration deviations from the respective bulk values are small. It follows that the bulk fluid domains can be regarded as 'Ohmic' media of uniform conductivities. In particular, the current density in the external bulk domain is, using the Einstein–Smoluchowski relation,

$$\frac{z^2e_*^2(D_*^+ + D_*^-)}{k_*T^*}c_*\boldsymbol{E}_*, \tag{3.2}$$

where $\boldsymbol{E}_*$ denotes the local electric field. The current density in the internal bulk domain is similar, with $M\bar{c}_*\bar{\boldsymbol{E}}_*$ replacing $c_*\boldsymbol{E}_*$, $\bar{\boldsymbol{E}}_*$ denoting the local field value.

With the Ohmic form (3.2), charge conservation in the bulk implies that the electric potentials of the conservative fields $\boldsymbol{E}_*$ and $\bar{\boldsymbol{E}}_*$ satisfy Laplace's equation. To obtain appropriate boundary conditions, we consider the conservation of charge in an infinitesimal slab-shaped control volume spanning the triple layer. Assuming that the contribution of tangential advection is small, we obtain an equality of radial bulk currents

$$c_*\boldsymbol{E}_* \cdot \hat{\boldsymbol{e}}_r \approx M\bar{c}_*\bar{\boldsymbol{E}}_* \cdot \hat{\boldsymbol{e}}_r, \tag{3.3}$$

where the fields $\boldsymbol{E}_*$ and $\bar{\boldsymbol{E}}_*$ are evaluated at the outer edges of the external and internal diffuse layers, respectively, and $\hat{\boldsymbol{e}}_r$ is a unit vector in the radial direction. Assuming furthermore that the tangential component of the electric field is approximately transversally uniform across the triple layer, we find that the tangential component of the bulk field is continuous across the 'macroscale interface.' Condition (3.3), in conjunction with that continuity condition, serves to uniquely determine the bulk electric fields. Upon identifying $M\bar{c}_*/c_*$ with the conductivity ratio R, these are the same as the fields calculated by Taylor (1966).

Since the applied field is assumed small compared with the Debye-layer field, the perturbation to the equilibrium Debye cloud due to passage of current is small.

https://doi.org/10.1017/jfm.2015.242 Published online by Cambridge University Press

This perturbation however is crucial since it results in a non-zero transversely integrated triple-layer charge: it is the action of the applied field on this 'apparent' non-equilibrium surface charge that gives rise to the dominant flow field. Indeed, applying the integral form of Gauss law to the same slab-shaped control volume yields the apparent charge

$$\Lambda_* \approx \epsilon_* \boldsymbol{E}_* \cdot \hat{\boldsymbol{e}}_r - S^{-1} \epsilon_* \bar{\boldsymbol{E}}_* \cdot \hat{\boldsymbol{e}}_r, \tag{3.4}$$

which is generally non-zero. In accordance with our underlying assumption (3.1) on the applied-field magnitude, the $O(\epsilon_* \mathscr{E}_*)$ magnitude of that charge is small compared with the $O(\epsilon_* \varphi_* \kappa_*)$ equilibrium triple-layer charge. Due to screening, however, the latter trivially vanishes. Given the assumption of a uniform tangential field in the triple layer, we find that the dominant flow is animated by the action of that field upon the perturbation to the equilibrium Debye cloud. We re-emphasize that the apparent charge is not concentrated on the genuine interface, but is radially distributed, corresponding to a perturbation to both the charge density in the two diffuse layers, and to the amount of adsorbed charge at the interface. Its distribution is not provided by the above argument, nor is it required when going on to determine the leading-order flow field.

Indeed, consider once again the same slab-shaped control volume. This time we employ an integral tangential–momentum balance. Ignoring the stresses acting on the side panels, this balance states that the macroscale jump $\tau_* - \bar{\tau}_*$ of the viscous shear stress is provided by the overall tangential electric force. Since the tangential field is approximately uniform across the triple layer, this force is just the product of the field and the total charge in the control volume, i.e. the apparent charge Λ_*. Thus,

$$\tau_* - \bar{\tau}_* \approx -\Lambda_* \boldsymbol{E}_* \cdot \hat{\boldsymbol{e}}_\theta, \tag{3.5}$$

where $\hat{\boldsymbol{e}}_\theta$ is a unit vector in the θ-direction. This is just the stress jump appearing in the leaky dielectric model, and as such it implies the familiar scale $\mathscr{U}_* = \epsilon_* a_* \mathscr{E}_*^2 / \mu^*$.

To determine the flow field, an additional macroscale condition is required. Given the action of the tangential field on the equilibrium Debye cloud, one may naïvely postulate that the missing condition is one of electro-osmotic slip. Indeed, while the action of the applied field on the screened 'equilibrium' charge does not result in a macroscale stress jump, it does result in a steep velocity profile that varies rapidly on the Debye scale and appears on the macroscale as a finite jump in the tangential velocity component. Electrokinetic theory implies however that the magnitude of that slip is $O(\epsilon_* \varphi_* \mathscr{E}_* / \mu_*)$; its ratio to the Taylor–Melcher velocity scale is $\varphi_* / a_* \mathscr{E}_*$, asymptotically small under assumption (3.1). It thus follows that on the macroscale (3.5) should be supplemented by a velocity continuity condition. The macro-flow problem thus coincides with that specified by Melcher & Taylor (1969).

It should be noted that the inevitable electro-osmotic slip gives rise to a small electrophoretic motion, which is of course absent in Taylor–Melcher model. It is also interesting to note that the Debye-scale electrokinetic flow exerts viscous stresses on the genuine interface which are stronger than (3.5). These strong stresses are however exactly balanced by the (equally strong) microscale electric stress associated with the action of the applied field on the charged interface. The macroscale stress-jump appearing in (3.5) thus represents a delicate balance of the perturbed stresses at the microscopic interface. This is compatible with the absence of electrokinetic parameters (such as the zeta potentials) in (3.5).

https://doi.org/10.1017/jfm.2015.242 Published online by Cambridge University Press

The goal of the preceding description, which is quite rough, is to provide an intuitive physical picture of the linkage between transport on the microscale and macroscale. This picture should hopefully aid the reader in following the mathematical analysis detailed in the sections that follow. We now turn to that analysis, starting with the systematic formulation of the physical problem described in § 2.

4. Problem formulation

We employ a dimensionless notation, using the standard electrokinetic scaling (Saville 1977). Length variables are normalized by a_*, ionic concentrations by $\mathscr{C}_*$, electric potentials by the thermal voltage

$$\varphi_* = \frac{k_* T_*}{z e_*} \tag{4.1}$$

(wherein $k_* T_*$ is the Boltzmann temperature and e_* the elementary charge), stress variables by the Maxwell scale $\epsilon_* \varphi_*^2 / a_*^2$, and velocity variables by $\epsilon_* \varphi_*^2 / \mu_* a_*$.

4.1. *Differential equations*

The pertinent variables in the suspending liquid are the ionic concentration $c^{\pm}$, the electric potential φ and the velocity field $\boldsymbol{u}$. These are governed by the differential equations of the standard electrokinetic model.

(*a*) Nernst–Planck ion conservation,

$$\boldsymbol{\nabla} \cdot \boldsymbol{j}^{\pm} + \alpha^{\pm} \boldsymbol{u} \cdot \boldsymbol{\nabla} c^{\pm} = 0, \tag{4.2}$$

wherein the molecular fluxes of cations and anions, respectively normalized by $D_*^{\pm} \mathscr{C}_* / a_*$, are due to diffusion and electro-migration,

$$\boldsymbol{j}^{\pm} = -\boldsymbol{\nabla} c^{\pm} \mp c^{\pm} \boldsymbol{\nabla} \varphi. \tag{4.3}$$

The ion drag coefficients

$$\alpha^{\pm} = \frac{\epsilon_* \varphi_*^2}{\mu_* D_*^{\pm}} \tag{4.4}$$

appearing in (4.2) are independent of both the drop size a_* and reference concentration $\mathscr{C}_*$. Moreover, because of the Stokes–Einstein relations, they are actually independent of the liquid viscosity μ^*; rather, they are simply proportional to the size of the ions. For typical ions in aqueous solutions, $\alpha^{\pm} \lesssim 0.5$ (Saville 1977).

(*b*) Poisson's equation,

$$-2\delta^2 \nabla^2 \varphi = c^+ - c^-, \tag{4.5}$$

wherein

$$\delta = \frac{1}{\kappa_* a_*} \tag{4.6}$$

is the dimensionless Debye thickness, in which the Debye width $1/\kappa_*$ is defined by

$$\kappa_*^2 = \frac{2 z e_* \mathscr{C}_*}{\epsilon_* \varphi_*}. \tag{4.7}$$

https://doi.org/10.1017/jfm.2015.242 Published online by Cambridge University Press

(*c*) Stokes equations, subject to Coulomb body forces,

$$\boldsymbol{\nabla}\cdot\boldsymbol{u}=0, \quad \boldsymbol{\nabla}p=\nabla^2\boldsymbol{u}+\nabla^2\varphi\boldsymbol{\nabla}\varphi, \tag{4.8a,b}$$

where p is the pressure field.

Within the drop we denote the ionic concentrations by $\bar{c}^{\pm}$, the electric potential by $\bar{\varphi}$, and the fluid velocity by $\bar{\boldsymbol{u}}$. These fields are governed by the following differential equations.

(*a*) Nernst–Planck ion conservation,

$$\boldsymbol{\nabla}\cdot\bar{\boldsymbol{j}}^{\pm}+\alpha^{\pm}\bar{\boldsymbol{u}}\cdot\boldsymbol{\nabla}\bar{c}^{\pm}=0, \tag{4.9}$$

where the molecular fluxes are again normalized by $D_*^{\pm}\mathscr{C}_*/a_*$:

$$\bar{\boldsymbol{j}}^{\pm}=M(\mp\bar{c}^{\pm}\boldsymbol{\nabla}\bar{\varphi}-\boldsymbol{\nabla}\bar{c}^{\pm}). \tag{4.10}$$

(*b*) Poisson's equation,

$$-2\delta^2S^{-1}\nabla^2\bar{\varphi}=\bar{c}^{+}-\bar{c}^{-}. \tag{4.11}$$

(*c*) Stokes equations, subject to Coulomb body forces,

$$\boldsymbol{\nabla}\cdot\bar{\boldsymbol{u}}=0, \quad \boldsymbol{\nabla}\bar{p}=M^{-1}\nabla^2\bar{\boldsymbol{u}}+S^{-1}\nabla^2\bar{\varphi}\boldsymbol{\nabla}\bar{\varphi}, \tag{4.12a,b}$$

wherein $\bar{p}$ is the drop-phase pressure field.

4.2. *Alternative formulation*

An alternative description is obtained through the use of the mean ('salt') concentration (normalized by $\mathscr{C}_*$) and volumetric charge density (normalized by $2ze_*\mathscr{C}_*$)

$$c=\tfrac{1}{2}(c^{+}+c^{-}), \quad q=\tfrac{1}{2}(c^{+}-c^{-}), \tag{4.13a,b}$$

instead of the ionic concentrations $c^{\pm}$. The 'salt flux' and 'current density,' defined by

$$\boldsymbol{j}=\frac{\boldsymbol{j}^{+}+\boldsymbol{j}^{-}}{2}, \quad \boldsymbol{i}=\frac{\boldsymbol{j}^{+}-\boldsymbol{j}^{-}}{2}, \tag{4.14a,b}$$

then adopt the forms (see (4.3))

$$\boldsymbol{j}=-\boldsymbol{\nabla}c-q\boldsymbol{\nabla}\varphi, \quad \boldsymbol{i}=-\boldsymbol{\nabla}q-c\boldsymbol{\nabla}\varphi. \tag{4.15a,b}$$

(Because $\boldsymbol{j}^{\pm}$ are normalized by different quantities, the quantities $\boldsymbol{j}$ and $\boldsymbol{i}$ do not possess the meaning of true flux quantities. Nonetheless, their use is convenient.) Mutual addition and subtraction of (4.2) yields the respective salt- and charge-conservation equations,

$$\boldsymbol{\nabla}\cdot\boldsymbol{j}+\frac{\alpha^{+}+\alpha^{-}}{2}\boldsymbol{u}\cdot\boldsymbol{\nabla}c+\frac{\alpha^{+}-\alpha^{-}}{2}\boldsymbol{u}\cdot\boldsymbol{\nabla}q=0, \tag{4.16}$$

$$\boldsymbol{\nabla}\cdot\boldsymbol{i}+\frac{\alpha^{+}-\alpha^{-}}{2}\boldsymbol{u}\cdot\boldsymbol{\nabla}c+\frac{\alpha^{+}+\alpha^{-}}{2}\boldsymbol{u}\cdot\boldsymbol{\nabla}q=0. \tag{4.17}$$

https://doi.org/10.1017/jfm.2015.242 Published online by Cambridge University Press

Note that Poisson's equation (4.5) now reads

$$q = -\delta^2 \nabla^2 \varphi. \tag{4.18}$$

Within the drop, the corresponding quantities

$$\bar{\boldsymbol{j}} = \frac{\bar{\boldsymbol{j}}^+ + \bar{\boldsymbol{j}}^-}{2}, \quad \bar{\boldsymbol{i}} = \frac{\bar{\boldsymbol{j}}^+ - \bar{\boldsymbol{j}}^-}{2} \tag{4.19a,b}$$

adopt the respective forms (see (4.10))

$$\bar{\boldsymbol{j}} = M(-\boldsymbol{\nabla}\bar{c} - \bar{q}\boldsymbol{\nabla}\bar{\varphi}), \quad \bar{\boldsymbol{i}} = M(-\boldsymbol{\nabla}\bar{q} - \bar{c}\boldsymbol{\nabla}\bar{\varphi}). \tag{4.20a,b}$$

Mutual addition and subtraction of (4.9) yields here the analogs of (4.16) and (4.17),

$$\boldsymbol{\nabla}\cdot\bar{\boldsymbol{j}} + \frac{\alpha^+ + \alpha^-}{2}\bar{\boldsymbol{u}}\cdot\boldsymbol{\nabla}\bar{c} + \frac{\alpha^+ - \alpha^-}{2}\bar{\boldsymbol{u}}\cdot\boldsymbol{\nabla}\bar{q} = 0, \tag{4.21}$$

$$\boldsymbol{\nabla}\cdot\bar{\boldsymbol{i}} + \frac{\alpha^+ - \alpha^-}{2}\bar{\boldsymbol{u}}\cdot\boldsymbol{\nabla}\bar{c} + \frac{\alpha^+ + \alpha^-}{2}\bar{\boldsymbol{u}}\cdot\boldsymbol{\nabla}\bar{q} = 0. \tag{4.22}$$

Last, Poisson's equation reads

$$\bar{q} = -\delta^2 S^{-1}\nabla^2\bar{\varphi}. \tag{4.23}$$

4.3. *Interfacial boundary conditions*

In writing the interfacial boundary conditions we denote the surface concentrations of cations and anions, normalized by $2\mathscr{C}_*/\kappa_*$, by $\Gamma^{\pm}$. With that definition, we find from (4.7) that

$$\Gamma^+ - \Gamma^- = \text{interfacial charge density (normalized by } \epsilon_*\kappa_*\varphi_*). \tag{4.24}$$

The boundary conditions are written using spherical polar coordinates (r, θ, ϖ), $r = 0$ coinciding with the drop centre and $\theta = 0$ pointing in the applied-field direction. Because of axial symmetry, all scalar fields are independent of the azimuthal angle ϖ. Moreover, the velocity fields admit the axially symmetry forms

$$\boldsymbol{u} = u\hat{\boldsymbol{e}}_r + v\hat{\boldsymbol{e}}_\theta, \quad \bar{\boldsymbol{u}} = \bar{u}\hat{\boldsymbol{e}}_r + \bar{v}\hat{\boldsymbol{e}}_\theta, \tag{4.25a,b}$$

with velocity components that are independent of ϖ. Similar forms apply to the ionic fluxes, the salt fluxes, and the current densities.

The conditions consist of the following.

(*a*) Ion conservation,

$$\hat{\boldsymbol{e}}_r\cdot(\boldsymbol{j}^{\pm} - \bar{\boldsymbol{j}}^{\pm}) + 2\delta\alpha^{\pm}\boldsymbol{\nabla}_s\cdot(\Gamma^{\pm}\boldsymbol{u}) = 0, \tag{4.26}$$

where the first term represents molecular flux from the bulk, and the second term represents surface convection (in which $\boldsymbol{\nabla}_s$ is the surface-gradient operator).

(*b*) Electric-potential continuity,

$$\varphi = \bar{\varphi}. \tag{4.27}$$

https://doi.org/10.1017/jfm.2015.242 Published online by Cambridge University Press

(*c*) The boundary form of Gauss law,

$$\Gamma^{+} - \Gamma^{-} = -\delta \left(\frac{\partial \varphi}{\partial r} - S^{-1} \frac{\partial \bar{\varphi}}{\partial r} \right). \tag{4.28}$$

(*d*) Impermeability,

$$u = \bar{u} = 0. \tag{4.29}$$

(*e*) Velocity continuity,

$$v = \bar{v}. \tag{4.30}$$

(*f*) Shear-stress balance,

$$\left(\frac{\partial v}{\partial r} - v \right) - M^{-1} \left(\frac{\partial \bar{v}}{\partial r} - \bar{v} \right) - \delta^{-1} \left(\Gamma^{+} - \Gamma^{-} \right) \frac{\partial \varphi}{\partial \theta} - \delta^{-1} \frac{\partial}{\partial \theta} (\Gamma^{+} + \Gamma^{-}) = 0, \tag{4.31}$$

where the last two terms respectively represent the electric shear stress and the Marangoni effect (see Baygents & Saville 1991).

In addition to conditions (4.26)–(4.31), the surface concentrations $\Gamma^{\pm}$ are subject to kinetic conditions governing ionic adsorption and desorption. Following Baygents & Saville (1989) we assume fast kinetics with a linear concentration dependence,

$$\Gamma^{\pm} = K^{\pm} c^{\pm} = \bar{K}^{\pm} \bar{c}^{\pm}, \tag{4.32}$$

wherein $(K^{\pm}, \bar{K}^{\pm})$ are adsorption coefficients, normalized by $2/\kappa_{*}$. As will become evident, $O(1)$ values of $(K^{\pm}, \bar{K}^{\pm})$ correspond to $O(1)$ zeta potentials.

4.4. *Additional conditions*

The boundary conditions at $r = 1$ are supplemented by appropriate far-field conditions. Thus, at large distances away from the drop the concentrations approach a unity value (in agreement with definition of $\mathscr{C}_{*}$ as the equilibrium concentration)

$$c \to 1, \quad q \to 0 \tag{4.33a,b}$$

and the electric field becomes uniform

$$\varphi \sim -\beta r \cos\theta, \tag{4.34}$$

wherein

$$\beta = \frac{a_{*} \mathscr{E}_{*}}{\varphi_{*}} \tag{4.35}$$

is the dimensionless magnitude of the applied field.

In contrast to standard electrohydrodynamic descriptions, the presence here of equilibrium charge necessitates the allowing of possible drop motion, say with velocity u^{∞}, relative to the otherwise quiescent liquid. In the comoving frame in which the preceding description is provided, this motion implies the far-field condition

$$\boldsymbol{u} \to -u^{\infty} \hat{\boldsymbol{i}} \tag{4.36}$$

where $\hat{\boldsymbol{i}}$ is a unit vector in the applied-field direction. The velocity u^{∞} is not *a priori* prescribed. Rather, it is determined from the condition that the drop is force free,

$$\oint \mathrm{d}A \, \hat{\boldsymbol{n}} \cdot \left\{ -p\boldsymbol{I} + \nabla \boldsymbol{u} + (\nabla \boldsymbol{u})^{\dagger} + \nabla \varphi \nabla \varphi - \tfrac{1}{2} \nabla \varphi \cdot \nabla \varphi \boldsymbol{I} \right\} = \boldsymbol{0}, \tag{4.37}$$

where both Newtonian and Maxwell stresses are accounted for. Here, $\boldsymbol{I}$ is the identity dyadic and $\dagger$ denotes tensor transposition. Note that condition (4.37) is trivially satisfied in the fore–aft symmetric Taylor–Melcher description.

https://doi.org/10.1017/jfm.2015.242 Published online by Cambridge University Press

5. The Baygents–Saville limit

We employ the Baygents–Saville limit where the diffuse-charge layers are thin and the electric field is strong

$$\delta \ll 1, \quad \beta \gg 1, \tag{5.1a,b}$$

with

$$\delta\beta \ll 1. \tag{5.2}$$

Since the applied electric field is $O(\beta)$, so too is the electric-potential distribution. We therefore postulate, subject to *a posteriori* verification, the following asymptotic expansion:

$$\varphi = \beta\varphi_{-1} + \cdots . \tag{5.3}$$

On the other hand, condition (4.33*a*) suggests that c remains $O(1)$ even under intense fields:

$$c = c_0 + \cdots . \tag{5.4}$$

In view of Poisson's equation (4.18) and (5.3), the volumetric charge density q is $O(\delta^2\beta)$, and is hence (see (5.2)) asymptotically small (consistently with (4.33*b*)). Thus, leading-order electro-neutrality prevails in the limit addressed herein. Finally, anticipating the Taylor–Melcher flow scaling, we postulate an $O(\beta^2)$ velocity field,

$$\boldsymbol{u} = \beta^2\boldsymbol{u}_{-2} + \cdots \tag{5.5}$$

with similar expansions for p and u^∞. Comparable expansions apply in the drop phase, namely

$$\bar{\varphi} = \beta\bar{\varphi}_{-1} + \cdots , \quad \bar{c} = \bar{c}_0 + \cdots , \quad \bar{q} = O(\delta^2\beta), \quad \bar{\boldsymbol{u}} = \beta^2\bar{\boldsymbol{u}}_{-2} + \cdots . \tag{5.6a–d}$$

With q and $\bar{q}$ being $O(\delta^2\beta)$, the electro-migration terms in the salt-flux expressions (4.15*a*) and (4.20*a*) are $O(\delta^2\beta^2)$ and hence asymptotically small compared with the $O(1)$ diffusive terms: see (5.2). We accordingly postulate

$$\boldsymbol{j} = \boldsymbol{j}_0 + \cdots , \quad \bar{\boldsymbol{j}} = \bar{\boldsymbol{j}}_0 + \cdots , \tag{5.7a,b}$$

wherein

$$\boldsymbol{j}_0 = -\boldsymbol{\nabla} c_0, \quad \bar{\boldsymbol{j}}_0 = -M\boldsymbol{\nabla}\bar{c}_0. \tag{5.8a,b}$$

On the other hand, the current densities are dominated by electro-migration, and are accordingly asymptotically large

$$\boldsymbol{i} = \beta\boldsymbol{i}_{-1} + \cdots , \quad \bar{\boldsymbol{i}} = \beta\bar{\boldsymbol{i}}_{-1} + \cdots ; \tag{5.9a,b}$$

here,

$$\boldsymbol{i}_{-1} = -c_0\boldsymbol{\nabla}\varphi_{-1}, \quad \bar{\boldsymbol{i}}_{-1} = -M\bar{c}_0\boldsymbol{\nabla}\bar{\varphi}_{-1}. \tag{5.10a,b}$$

The leading $O(\beta^2)$ salt balances (4.16) and (4.21) are dominated by convection,

$$\boldsymbol{u}_{-2}\cdot\boldsymbol{\nabla} c_0 = 0, \quad \bar{\boldsymbol{u}}_{-2}\cdot\boldsymbol{\nabla}\bar{c}_0 = 0. \tag{5.11a,b}$$

It follows that c_0 and $\bar{c}_0$ are constant along the streamlines of the respective leading-order flow fields $\boldsymbol{u}_{-2}$ and $\bar{\boldsymbol{u}}_{-2}$. Since we anticipate at leading order to obtain Taylor's

https://doi.org/10.1017/jfm.2015.242 Published online by Cambridge University Press

quadrupolar flow structure, we make the *a priori* assumption that the streamlines in the suspending liquid are open, extending to infinity. Condition (4.33*a*) thus implies

$$c_0 \equiv 1. \tag{5.12}$$

Given this result, it is readily verified that all higher-order corrections to c_0 trivially vanish; we therefore conclude that

$$c \sim 1 + \text{exponentially-small terms}. \tag{5.13}$$

Of course, such an argument cannot be employed for the calculation of the salt concentration $\bar{c}_0$ inside the drop. In appendix A we nonetheless find that $\bar{c}_0$ is uniform as well. Its value, however, is yet undetermined.

Because of the small charge density in the bulk, the leading $O(\beta)$ charge balances (4.17) and (4.22) are dominated by conduction

$$\boldsymbol{\nabla}\cdot\boldsymbol{i}_{-1} = 0, \quad \boldsymbol{\nabla}\cdot\bar{\boldsymbol{i}}_{-1} = 0. \tag{5.14a,b}$$

Substitution of (5.10*a*) and use of the $O(1)$ salt uniformity, we obtain Laplace's equations in both phases.

$$\nabla^2\varphi_{-1} = 0, \quad \nabla^2\bar{\varphi}_{-1} = 0. \tag{5.15a,b}$$

If follows that Coulomb body forces do not affect the leading $O(\beta^2)$ momentum balances

$$\boldsymbol{\nabla}p_{-2} = \nabla^2\boldsymbol{u}_{-2}, \quad \boldsymbol{\nabla}\bar{p}_{-2} = M^{-1}\nabla^2\bar{\boldsymbol{u}}_{-2}, \tag{5.16a,b}$$

which, together with the respective continuity equations,

$$\boldsymbol{\nabla}\cdot\boldsymbol{u}_{-2} = 0, \quad \boldsymbol{\nabla}\cdot\bar{\boldsymbol{u}}_{-2} = 0, \tag{5.17a,b}$$

govern the leading $O(\beta^2)$ flow.

The preceding leading-order equations are supplemented by the far-field conditions,

$$\varphi_{-2} \sim -r\cos\theta, \quad \boldsymbol{u}_{-2} \to -u^{\infty}_{-2}\hat{\boldsymbol{\imath}}, \tag{5.18a,b}$$

and the leading $O(\beta^2)$ force-free condition

$$\oint \mathrm{d}A\,\hat{\boldsymbol{n}}\cdot\left\{-p_{-2}\boldsymbol{I} + \boldsymbol{\nabla}\boldsymbol{u}_{-2} + (\boldsymbol{\nabla}\boldsymbol{u}_{-2})^{\dagger} + \boldsymbol{\nabla}\varphi_{-1}\boldsymbol{\nabla}\varphi_{-1} - \tfrac{1}{2}\boldsymbol{\nabla}\varphi_{-1}\cdot\boldsymbol{\nabla}\varphi_{-1}\boldsymbol{I}\right\} = \boldsymbol{0}, \tag{5.19}$$

which, in principle, is affected by both Newtonian and Maxwell stresses.

Of course, the electro-neutral approximation derived in the limit (5.1) and (5.2) is incompatible with the boundary conditions (4.26)–(4.32). That non-uniformity can be traced to the singular nature of the small-δ limit, manifested by the multiplication of the highest derivative in (4.18) and (4.23) by a small parameter. Equations (5.3)–(5.19) thus only represent the outer ('bulk') regions in an inner–outer decomposition of the pertinent fluid domains. The corresponding inner regions are the two boundary (Debye) layers of width $O(\delta)$ formed about the interface $r = 1$. These are addressed next.

https://doi.org/10.1017/jfm.2015.242 Published online by Cambridge University Press

6. Debye-layer analysis

The Debye layers about $r=1$ are resolved using the stretched radial coordinate

$$Z=\frac{r-1}{\delta}. \tag{6.1}$$

Hereafter, the sphere $r=1$ is reinterpreted as an effective boundary at which asymptotic matching effectively takes place, as opposed to the genuine interface $Z=0$.

We employ capital letters to denote Debye-layer fields, using the generic transformation

$$f(r,\theta)=F(Z,\theta),\quad \bar{f}(r,\theta)=\bar{F}(Z,\theta). \tag{6.2a,b}$$

Using the volumetric charge densities Q and $\bar{Q}$, we define the effective 'surface-charge' densities (normalized by $2ze_*\mathscr{C}_*/\kappa_*$) of the two diffuse layers,

$$\mathscr{Q}=\int_0^\infty Q\,\mathrm{d}Z,\quad \bar{\mathscr{Q}}=\int_{-\infty}^0 \bar{Q}\,\mathrm{d}Z, \tag{6.3a,b}$$

which are accordingly functions of θ alone. We additionally define the apparent surface-charge density, normalized by $2ze_*\mathscr{C}_*/\kappa_*$

$$\Lambda=\Gamma^+-\Gamma^-+\mathscr{Q}+\bar{\mathscr{Q}}. \tag{6.4}$$

In view of (4.7), the normalizing scale $2ze_*\mathscr{C}_*/\kappa_*$ is equal to $\epsilon_*\kappa_*\varphi_*$, used for normalizing the surface-charge density $\Gamma^+-\Gamma^-$ on the literal interface, see (4.24).

6.1. *Expansions*

Consider now the asymptotic expansions in the exterior Debye layer (with similar expansions holding in the interior layer). We postulate the following expansion of the ionic concentrations

$$C^\pm=C^\pm_{0,0}+\delta\beta C^\pm_{1,-1}+\cdots, \tag{6.5}$$

with similar expansions for C and Q. We also postulate the electric-potential expansion

$$\Phi=\beta\Phi_{0,-1}+\Phi_{0,0}+\delta\beta\Phi_{1,-1}+\cdots, \tag{6.6}$$

and the following expansion of radial ionic fluxes

$$\hat{\boldsymbol{e}}_r\cdot\boldsymbol{J}^\pm=\beta J^\pm_{0,-1}+\delta\beta^2 J^\pm_{1,-2}+\delta\beta J^\pm_{1,-1}+\cdots, \tag{6.7}$$

which imply, in turn, for the radial salt flux and current density,

$$\hat{\boldsymbol{e}}_r\cdot\boldsymbol{J}=\beta J_{0,-1}+\delta\beta^2 J_{1,-2}+\delta\beta J_{1,-1}+\cdots, \tag{6.8}$$

$$\hat{\boldsymbol{e}}_r\cdot\boldsymbol{I}=\beta I_{0,-1}+\delta\beta^2 I_{1,-2}+\delta\beta I_{1,-1}+\cdots. \tag{6.9}$$

Following (5.5), we also propose for the tangential velocity

$$V=\beta^2 V_{0,-2}+\beta V_{0,-1}+\delta\beta^2 V_{1,-2}+\cdots. \tag{6.10}$$

https://doi.org/10.1017/jfm.2015.242 Published online by Cambridge University Press

The continuity equation (4.8*a*) in conjunction with the impermeability condition (4.29) then implies an $O(\delta\beta^2)$ radial velocity

$$U \sim O(\delta\beta^2). \tag{6.11}$$

Note that the prefactors in the various expansions of velocity and flux-like variables always involve β; this is plausible since in the absence of an applied field the system is in equilibrium with no flow or net fluxes. It is also worth noting that the asymptotic limit (5.1) and (5.2) does not determine the magnitude of the prefactor $\delta\beta^2$ relative to unity; this however does not pose any restriction on the resulting analysis.

In addition to the expansions within the fluid domains, we also need to present asymptotic expansions of the interfacial ionic concentrations. In view of the kinetic conditions (4.32), we anticipate similar expansions as those of the Debye-layer concentrations, see (6.5):

$$\Gamma^{\pm} = \Gamma^{\pm}_{0,0} + \delta\beta\,\Gamma^{\pm}_{1,-1} + \cdots. \tag{6.12}$$

Note that $\mathscr{Q}$ and $\bar{\mathscr{Q}}$, and hence also Λ, possess similar expansions.

6.2. *Preliminary results*

From the $O(\beta)$ balance of Poisson's equation we find $\partial^2\Phi_{0,-1}/\partial Z^2 = 0$, implying that $\Phi_{0,-1}$ must grow linearly with Z: $\Phi_{0,-1} = A(\theta)Z + B(\theta)$. Asymptotic matching with the $O(\beta)$ bulk potential reveals that $A = 0$; as $\Phi_{0,-1}$ is independent of Z, it is simply an extrapolation of the bulk potential φ_{-1}. Similarly, $\bar{\Phi}_{0,-1}$ is an extrapolation of the bulk potential $\bar{\varphi}_{-1}$ within the drop. We write these results in the form

$$\Phi_{0,-1} \equiv \varphi_{-1}, \quad \bar{\Phi}_{0,-1} \equiv \bar{\varphi}_{-1}; \tag{6.13a,b}$$

hereafter, bulk variables appearing in Debye-scale equations are understood to be evaluated at the macroscale boundary $r = 1$. The microscale continuity condition (4.27) at $Z = 0$ then furnishes the effective continuity condition

$$\varphi_{-1} = \bar{\varphi}_{-1}. \tag{6.14}$$

With transverse non-uniformities in the electric potential appearing only at $O(1)$, the radial Debye-layer electric fields retain their $O(\delta^{-1})$ equilibrium scaling, just as in standard electrokinetic phenomena under moderate applied fields (Yariv 2009).

Consider now the momentum balance in the radial direction, where the $O(\delta^{-1}\beta^2)$ viscous stresses are dominated by the $O(\delta^{-3})$ Coulomb body forces. This implies that the Z-derivatives of P and $\bar{P}$ are $O(\delta^{-2})$: the $O(\delta^{-2})$ pressure field is accordingly transversely non-uniform. Moreover, since the pressure variations in the bulk are at most $O(\beta^2)$, asymptotically smaller than δ^{-2}, large-Z matching excludes the possibility of a transversely-uniform Debye-layer pressure term which is $\gg \delta^{-2}$.

The momentum balances in the tangential direction, at leading $O(\delta^{-2}\beta^2)$, is accordingly unaffected by the Debye-layer pressure; they merely read

$$\frac{\partial^2 V_{0,-2}}{\partial Z^2} = 0, \quad \frac{\partial^2 \bar{V}_{0,-2}}{\partial Z^2} = 0. \tag{6.15a,b}$$

https://doi.org/10.1017/jfm.2015.242 Published online by Cambridge University Press

Asymptotic matching with the leading $O(\beta^2)$ bulk flow then reveals that $V_{0,-2}$ and $\bar{V}_{0,-2}$ are transversely uniform; just as the leading-order potentials, they constitute extrapolations of the corresponding bulk variables (see (4.25)):

$$V_{0,-2} \equiv v_{-2}, \quad \bar{V}_{0,-2} \equiv \bar{v}_{-2}. \tag{6.16a,b}$$

The microscale continuity condition (4.30) at $Z = 0$ then results in the effective continuity condition

$$v_{-2} = \bar{v}_{-2} \quad \text{at } r = 1, \tag{6.17}$$

governing the bulk fields. This condition is supplemented by the effective impermeability condition

$$u_{-2} = \bar{u}_{-2} = 0 \quad \text{at } r = 1, \tag{6.18}$$

which simply follows from the Debye scaling (6.11) of the radial velocities.

With the transversely uniform leading-order velocities (6.16), the continuity equation implies that the leading $O(\delta\beta^2)$ radial component must vary linearly with Z. It then follows from the radial momentum balance that the pressure associated with the leading-order flow is only $O(\delta\beta^2)$, asymptotically smaller than the $O(\delta^{-2})$ pressure associated with the combination of $O(1)$ volume-charge density and $O(\delta^{-1})$ transverse electric field in the Debye layer, which we consider next.

6.3. *Leading-order Debye cloud*

The presumed absence of $O(\delta^{-1})$ radial ionic fluxes implies (see (6.7))

$$\frac{\partial C^{\pm}_{0,0}}{\partial Z} \pm C^{\pm}_{0,0}\frac{\partial \Phi_{0,0}}{\partial Z} = 0, \quad \frac{\partial \bar{C}^{\pm}_{0,0}}{\partial Z} \pm \bar{C}^{\pm}_{0,0}\frac{\partial \bar{\Phi}_{0,0}}{\partial Z} = 0. \tag{6.19a,b}$$

Integration in conjunction with large-Z asymptotic matching furnishes the Boltzmann distributions

$$C^{\pm}_{0,0} = \mathrm{e}^{\mp\Psi}, \quad \bar{C}^{\pm}_{0,0} = \bar{c}_0\mathrm{e}^{\mp\bar{\Psi}}, \tag{6.20a,b}$$

wherein $\bar{c}_0$ is the uniform salt concentration within drop (yet to be determined) and

$$\Psi = \Phi_{0,0} - \varphi_0, \quad \bar{\Psi} = \bar{\Phi}_{0,0} - \bar{\varphi}_0 \tag{6.21a,b}$$

are the excess potentials within the suspending liquid and the drop, respectively. In view of the matching requirement, these variables must vanish as $Z \to \pm\infty$, respectively. The charge densities associated with (6.20) are

$$Q_{0,0} = -\sinh\Psi, \quad \bar{Q}_{0,0} = -\bar{c}_0\sinh\bar{\Psi}. \tag{6.22a,b}$$

Substitution into the $O(1)$ balances of Poisson's equations

$$\frac{\partial^2\Psi}{\partial Z^2} = -Q_{0,0}, \quad \frac{\partial^2\bar{\Psi}}{\partial Z^2} = -S\bar{Q}_{0,0}, \tag{6.23a,b}$$

followed by integration (using the decay conditions at $\pm\infty$) yields the first-order equations

$$\frac{\partial\Psi}{\partial Z} = -2\sinh\frac{\Psi}{2}, \quad \frac{\partial\bar{\Psi}}{\partial Z} = 2\sqrt{S\bar{c}_0}\sinh\frac{\bar{\Psi}}{2}. \tag{6.24a,b}$$

https://doi.org/10.1017/jfm.2015.242 Published online by Cambridge University Press

We define the zeta potentials as the leading-order voltage drops between the interface and the respective bulk values,

$$\zeta = \Psi(Z=0), \quad \bar{\zeta} = \bar{\Psi}(Z=0). \tag{6.25a,b}$$

Using (6.20), the ionic concentrations about $Z=0$ are

$$C_0^{\pm}(Z=0^+) = \mathrm{e}^{\mp\zeta}, \quad \bar{C}_0^{\pm}(Z=0^+) = \bar{c}_0\mathrm{e}^{\mp\bar{\zeta}}. \tag{6.26a,b}$$

The kinetic conditions (4.32) thus read at $O(1)$

$$\Gamma_{0,0}^{\pm} = K^{\pm}\mathrm{e}^{\mp\zeta} = \bar{K}^{\pm}\bar{c}_0\mathrm{e}^{\mp\bar{\zeta}}, \tag{6.27}$$

providing four equations for the five unknowns $\Gamma_{0,0}^{\pm}$, ζ, $\bar{\zeta}$ and $\bar{c}_0$. An additional equation is provided by the $O(1)$ balance of Gauss law's (4.28)

$$\Gamma_{0,0}^{+} - \Gamma_{0,0}^{-} = -\frac{\partial\Psi}{\partial Z} + S^{-1}\frac{\partial\bar{\Psi}}{\partial Z} \quad \text{at } Z=0, \tag{6.28}$$

which, upon substitution of (6.24), becomes

$$\Gamma_{0,0}^{+} - \Gamma_{0,0}^{-} = 2\left(\sinh\frac{\zeta}{2} + \sqrt{\bar{c}_0/S}\sinh\frac{\bar{\zeta}}{2}\right). \tag{6.29}$$

Since (6.27) and (6.29) are algebraic equations, $\Gamma_{0,0}^{\pm}$ and the zeta potentials ζ and $\bar{\zeta}$ are independent of θ (and then so are Ψ and $\bar{\Psi}$). These variables, together with $\bar{c}_0$, depend only upon the adsorption coefficients ($K^{\pm}$, $\bar{K}^{\pm}$) and the permittivity ratio S. Specifically, (6.27) readily yield

$$\bar{c}_0 = \sqrt{\frac{K^+K^-}{\bar{K}^+\bar{K}^-}}. \tag{6.30}$$

Finally, transverse integration of (6.22) using (6.24) yields

$$\mathscr{Q}_{0,0} = -2\sinh\frac{\zeta}{2}, \quad \bar{\mathscr{Q}}_{0,0} = -2\sqrt{\bar{c}_0/S}\sinh\frac{\zeta}{2}. \tag{6.31a,b}$$

Substitution of these results and (6.29) into (6.4) yields zero apparent charge at $O(1)$

$$\Lambda_{0,0} = 0, \tag{6.32}$$

representing the expected screening of the interfacial charge by the surrounding Debye layers.

Of course, the effective conditions (6.14) and (6.17) and (6.18) are insufficient to determine the leading-order electric field and fluid flow. To obtain the requisite additional boundary conditions, we must go beyond leading-order analysis in the Debye layers.

7. Effective boundary conditions

We now go beyond the leading-order structure of the Debye layers, where asymptotic matching serves to provide effective boundary conditions governing the bulk fields.

https://doi.org/10.1017/jfm.2015.242 Published online by Cambridge University Press

7.1. *Effective current continuity*

Within the Debye layer, non-zero transverse ionic fluxes appear at $O(\beta)$. The $O(\delta^{-1}\beta)$ balances of the Nernst–Planck equations (4.2) read

$$\frac{\partial J^{\pm}_{0,-1}}{\partial Z}=0, \quad \frac{\partial \bar{J}^{\pm}_{0,-1}}{\partial Z}=0. \tag{7.1a,b}$$

Thus, the $O(\beta)$ fluxes are transversely uniform (but may depend upon θ). Consider now the leading $O(\beta)$ balances of the surface conservation equations (4.26). Since the advection term is only $O(\delta\beta^2)$, it is subdominant to the $O(\beta)$ diffusive fluxes (see (5.2)). We accordingly find:

$$J^{\pm}_{0,-1}=\bar{J}^{\pm}_{0,-1} \quad \text{at } Z=0. \tag{7.2}$$

In view of the transversal uniformity of $J^{\pm}_{0,-1}$ and $\bar{J}^{\pm}_{0,-1}$, the left-hand side may be evaluated at any Z (>0) and the right-hand side may be evaluated at any Z (<0). Mutual subtraction thus implies

$$I_{0,-1}=\bar{I}_{0,-1} \tag{7.3}$$

where, again, the left-hand side may be evaluated at any $Z(>0)$ and the right-hand side may be evaluated at any $Z(<0)$. This current-density constancy, in conjunction with the requisite matching with the outer currents, yields an effective current-continuity condition

$$\hat{\boldsymbol{e}}_r\cdot\boldsymbol{i}_{-1}=\hat{\boldsymbol{e}}_r\cdot\bar{\boldsymbol{i}}_{-1}. \tag{7.4}$$

Specifically, substitution of (5.10) and (5.12) yields the effective condition

$$\frac{\partial\varphi_{-1}}{\partial r}=M\bar{c}_0\frac{\partial\bar{\varphi}_{-1}}{\partial r}. \tag{7.5}$$

With the effective conditions (6.14) and (7.5), the outer potentials φ_{-1} and $\bar{\varphi}_{-1}$ are completely determined. Note that charge convection does not appear in the effective surface-charge balance (7.5).

7.2. *Effective Gauss-type condition*

Consider now Poisson's equation (4.18) at $O(\delta\beta)$:

$$-\frac{\partial^2\Phi_{1,-1}}{\partial Z^2}=Q_{1,-1}, \quad -S^{-1}\frac{\partial^2\bar{\Phi}_{1,-1}}{\partial Z^2}=\bar{Q}_{1,-1}. \tag{7.6a,b}$$

We integrate these equations with respect to Z, the first from 0 to ∞ and the second from $-\infty$ to 0. Use of the matching requirements

$$\frac{\partial\Phi_{1,-1}}{\partial Z}(Z\to\infty)\to\frac{\partial\varphi_{-1}}{\partial r}, \quad \frac{\partial\bar{\Phi}_{1,-1}}{\partial Z}(Z\to-\infty)\to\frac{\partial\bar{\varphi}_{-1}}{\partial r}, \tag{7.7a,b}$$

then yields

$$-\frac{\partial\varphi_{-1}}{\partial r}+\frac{\partial\Phi_{1,-1}}{\partial Z}(Z=0)=\mathscr{Q}_{1,-1}, \tag{7.8}$$

https://doi.org/10.1017/jfm.2015.242 Published online by Cambridge University Press

$$-S^{-1}\frac{\partial\bar{\Phi}_{1,-1}}{\partial Z}(Z=0)+S^{-1}\frac{\partial\bar{\varphi}_{-1}}{\partial r}=\bar{\mathscr{Q}}_{1,-1}. \tag{7.9}$$

The derivatives at $Z=0$ are related by the $O(\delta\beta)$ balance of Gauss's condition (4.28), namely:

$$\Gamma^{+}_{1,-1}-\Gamma^{-}_{1,-1}=-\frac{\partial\Phi_{1,-1}}{\partial Z}+S^{-1}\frac{\partial\bar{\Phi}_{1,-1}}{\partial Z}\quad\text{at } Z=0. \tag{7.10}$$

Use of (6.4) thus provides the macroscale apparent surface charge at $O(\delta\beta)$

$$\Lambda_{1,-1}=\frac{\partial\varphi_{-1}}{\partial r}-S^{-1}\frac{\partial\bar{\varphi}_{-1}}{\partial r}. \tag{7.11}$$

In view of (6.32), this is the leading-order apparent net charge.

7.3. *Flow*

Since $V_{0,-2}$ is independent of Z, the first non-trivial balance of the tangential momentum balance is associated with the leading $O(\beta)$ correction to the Debye-scale velocity. Upon making use of (6.13), this balance yields at $O(\delta^{-2}\beta)$:

$$\frac{\partial^2V_{0,-1}}{\partial Z^2}=-\frac{\mathrm{d}^2\Psi}{\mathrm{d}Z^2}\frac{\partial\varphi_{-1}}{\partial\theta},\quad M^{-1}\frac{\partial^2\bar{V}_{0,-1}}{\partial Z^2}=-S^{-1}\frac{\mathrm{d}^2\bar{\Psi}}{\mathrm{d}Z^2}\frac{\partial\varphi_{-1}}{\partial\theta}. \tag{7.12a,b}$$

(Note that at this order there are no Debye-scale tangential pressure gradients.) A single integration yields

$$\frac{\partial V_{0,-1}}{\partial Z}=-\frac{\mathrm{d}\Psi}{\mathrm{d}Z}\frac{\partial\varphi_{-1}}{\partial\theta},\quad M^{-1}\frac{\partial\bar{V}_{0,-1}}{\partial Z}=-S^{-1}\frac{\mathrm{d}\bar{\Psi}}{\mathrm{d}Z}\frac{\partial\bar{\varphi}_{-1}}{\partial\theta}, \tag{7.13a,b}$$

where the integration constants (functions of θ) must vanish by asymptotic matching with the $O(\beta^2)$ shear rate in the bulk. Consider now the leading $O(\delta^{-1}\beta)$ balance of the shear-stress jump condition (4.31),

$$\frac{\partial V_{0,-1}}{\partial Z}-M^{-1}\frac{\partial\bar{V}_{0,-1}}{\partial Z}=(\Gamma^{+}_{0,0}-\Gamma^{-}_{0,0})\frac{\partial\varphi_{-1}}{\partial\theta}\quad\text{at } Z=0. \tag{7.14}$$

Upon substitution of (7.13) and Gauss's condition (6.28), it is evident that this condition is trivially satisfied.

We accordingly address the leading $O(\delta^{-1}\beta^2)$ correction of the tangential momentum balances, associated with transverse variations of the $O(\delta\beta^2)$ tangential velocities. In view of (6.13) and the $O(\delta\beta)$ balance of Poisson's equation, and given the absence of $O(\delta^{-1}\beta^2)$ tangential pressure gradients, these balances read

$$\frac{\partial^2V_{1,-2}}{\partial Z^2}=Q_{1,-1}\frac{\partial\varphi_{-1}}{\partial\theta},\quad M^{-1}\frac{\partial^2\bar{V}_{1,-2}}{\partial Z^2}=\bar{Q}_{1,-1}\frac{\partial\bar{\varphi}_{-1}}{\partial\theta}. \tag{7.15a,b}$$

Respective integration of these equations from 0 to ∞ and from $-\infty$ to 0, in conjunction with the matching conditions

$$\frac{\partial V_{1,-2}}{\partial Z}(Z\to\infty)=\frac{\partial v_{-2}}{\partial r},\quad\frac{\partial\bar{V}_{1,-2}}{\partial Z}(Z\to-\infty)=\frac{\partial\bar{v}_{-2}}{\partial r} \tag{7.16a,b}$$

https://doi.org/10.1017/jfm.2015.242 Published online by Cambridge University Press

yields

$$\frac{\partial v_{-2}}{\partial r} - \frac{\partial V_{1,-2}}{\partial Z}(Z=0) = \mathscr{Q}_{1,-1}\frac{\partial \varphi_{-1}}{\partial \theta}, \tag{7.17a}$$

$$M^{-1}\left[\frac{\partial \bar{V}_{1,-2}}{\partial Z}(Z=0) - \frac{\partial \bar{v}_{-2}}{\partial r}\right] = \bar{\mathscr{Q}}_{1,-1}\frac{\partial \bar{\varphi}_{-1}}{\partial \theta}. \tag{7.17b}$$

We now consider the $O(\beta^2)$ balance of the shear-stress jump condition (4.31):

$$\frac{\partial V_{-2,1}}{\partial Z} - v_{-2} - M^{-1}\left(\frac{\partial \bar{V}_{-2,1}}{\partial Z} - \bar{v}_{-2}\right) = (\Gamma^{+}_{1,-1} - \Gamma^{-}_{1,-1})\frac{\partial \varphi_{-1}}{\partial \theta} \quad \text{at } Z=0. \tag{7.18}$$

Substituting (7.17) while making use of (6.14) and the definition (6.4) furnishes the effective shear-stress jump condition

$$\frac{\partial v_{-2}}{\partial r} - v_{-2} - M^{-1}\left(\frac{\partial \bar{v}_{-2}}{\partial r} - \bar{v}_{-2}\right) = \Lambda_{1,-1}\frac{\partial \varphi_{-1}}{\partial \theta}, \tag{7.19}$$

which entail the apparent charge $\Lambda_{1,-1}$, itself provided by the effective Gauss condition (7.11). Since condition (7.19) together with (6.17) and (6.18) is sufficient to determine the bulk Stokes flows, we have successfully obtained a closed macroscale model.

7.4. *Conductivity ratio*

The effective condition (7.5) is expressed in terms of $M\bar{c}_0$. This product is actually equal to the conductivity ratio R used by Melcher & Taylor (1969). To see that, we note that the dimensional current densities in the suspending and drop phases are respectively provided by the expressions

$$ze_*\frac{D^{+}_{*}\mathscr{C}_*}{a_*}\boldsymbol{j}^{+} - ze_*\frac{D^{-}_{*}\mathscr{C}_*}{a_*}\boldsymbol{j}^{-}, \quad ze_*\frac{D^{+}_{*}\mathscr{C}_*}{a_*}\bar{\boldsymbol{j}}^{+} - ze_*\frac{D^{-}_{*}\mathscr{C}_*}{a_*}\bar{\boldsymbol{j}}^{-}. \tag{7.20a,b}$$

(As already mentioned, neither of the dimensionless quantities $\boldsymbol{i}$ nor $\bar{\boldsymbol{i}}$ represents a true current density because of the different non-dimensionalization of cationic and anionic fluxes.) These densities may be expressed in terms of $\boldsymbol{j}$ and $\boldsymbol{i}$ through (4.14). As $\boldsymbol{i}$ is $O(\beta)$ while $\boldsymbol{j}$ is asymptotically smaller, we find that at leading $O(\beta)$ the ionic fluxes $\boldsymbol{j}^{\pm}$ are respectively given by $\pm\boldsymbol{i}$ (and, similarly, $\bar{\boldsymbol{j}}^{\pm}$ are respectively given by $\pm\bar{\boldsymbol{i}}$). Moreover, at that leading order $\boldsymbol{i} = -\boldsymbol{\nabla}\varphi$ and $\bar{\boldsymbol{i}} = -M\bar{c}_0\boldsymbol{\nabla}\bar{\varphi}$, see (5.10) and (5.12). Thus, the dimensional current densities (7.20) in the suspending and drop phases are respectively proportional to the dimensional electric fields, $-(\varphi_*/a_*)\boldsymbol{\nabla}\varphi$ and $-(\varphi_*/a_*)\boldsymbol{\nabla}\bar{\varphi}$, the proportionality coefficients being

$$ze_*\frac{\mathscr{C}_*}{\varphi_*}(D^{+}_{*} + D^{-}_{*}), \quad M\bar{c}_0 ze_*\frac{\mathscr{C}_*}{\varphi_*}(D^{+}_{*} + D^{-}_{*}). \tag{7.21a,b}$$

Accordingly, the respective expressions (7.21) constitute the conductivities of the suspending fluid and the drop. The ratio of the drop conductivity to that of the suspending electrolyte is

$$R = M\bar{c}_0. \tag{7.22}$$

https://doi.org/10.1017/jfm.2015.242 Published online by Cambridge University Press

7.5. *Electrophoretic velocity*

We now consider the leading-order electrophoretic velocity. We first observe that the structure governing the harmonic $O(\beta)$ potential φ_{-1} does not allow for a monopole term. Indeed, the problem governing the $O(\beta)$ potentials φ_{-1} and $\bar{\varphi}_{-1}$ is uncoupled to the flow, and is animated by the inhomogeneous far-field condition (5.18*a*); so, aside from an additive constant, both potentials must be proportional to $\cos\theta$. In the absence of a monopole term, and with a far-field approach to a uniform field, the electric field associated with φ_{-1} cannot result in a net electrostatic force at $O(\beta^2)$, see Rivette & Baygents (1996). The force acting on the drop at that asymptotic order in solely contributed by Newtonian stresses associated with leading-order $O(\beta^2)$ flow (represented by the first two terms in the integrand of (5.19)). Since that flow (as well as the comparable flow within the drop) is governed by the homogeneous Stokes equations (5.16) with a constraint of a zero hydrodynamic force, symmetry arguments imply that u^{∞} must vanish at $O(\beta^2)$:

$$u^{\infty}_{-2} = 0. \tag{7.23}$$

As discussed in § 10.5, drop electrophoresis does appear at a higher asymptotic order.

7.6. *Effective normal-stress jump*

In the preceding derivation, the drop shape was taken to be spherical. This is tantamount to assuming a large surface-tension coefficient (small capillary number). The preceding results thus correspond to the leading-order description in a formal expansion in the small capillary number. The leading-order deviation from sphericity can be readily determined once the normal-stress jump associated with the leading-order description is calculated (Leal 2007).

This approach was indeed used extensively in electrohydrodynamic analyses (Torza, Cox & Mason 1971), where the normal-stress jump was evaluated using the Taylor–Melcher model. This raises a fundamental question, since the drop deformation is actually affected by the microscale stresses at the genuine interface: is it legitimate to employ the macroscale stresses toward calculation of that deformation?

In appendix B we evaluate the microscale stress jump across the interface and show that it coincides with the one 'naïvely' evaluated using the macroscale model. The calculation scheme used in applications of the Taylor–Melcher model is thus substantiated.

8. Recapitulation

We have obtained a closed macroscale formulation consisting of bulk differential equations and effective boundary conditions. These allow to calculate the leading-order bulk potentials φ_{-1} and $\bar{\varphi}_{-1}$, apparent surface charge density $\Lambda_{1,-1}$, and bulk velocity fields $\boldsymbol{u}_{-2}$ and $\bar{\boldsymbol{u}}_{-2}$. No electrophoresis occurs at the leading-order flow problem, which accordingly describes the flow about a stationary drop.

Recall that in the present electrokinetic normalization, electric potentials are scaled by φ_*, velocities by $\epsilon_*\varphi_*^2/\mu_* a_*$, and surface-charge densities by $\epsilon_*\kappa_*\varphi_*$. In this dimensionless description, the electric potential is $O(\beta)$, the fluid velocity is $O(\beta^2)$, and the apparent surface-charge density is $O(\delta\beta)$. These correspond to the respective dimensional scales

$$a_*\mathscr{E}_*, \quad \epsilon_* a_* \mathscr{E}_*^2/\mu_*, \quad \epsilon_*\mathscr{E}_*. \tag{8.1a–c}$$

We have therefore recovered the leaky dielectric scaling of Melcher & Taylor (1969).

https://doi.org/10.1017/jfm.2015.242 Published online by Cambridge University Press

To recapitulate the macroscale model in a simple form we now use (8.1) to respectively normalize the electric potentials, the fluid velocity fields (with the pressure consistently normalized by $\epsilon_* \mathscr{E}_*^2$) and the surface-charge density. We summarize below the leading-order macroscale problem using the above leaky dielectric scaling, decorating the new dimensionless variables with a prime.

The electric potentials φ' and $\bar{\varphi}'$ satisfy Laplace's equation (cf. (5.15)),

$$\nabla^2 \varphi' = 0, \quad \nabla^2 \bar{\varphi}' = 0, \tag{8.2a,b}$$

the continuity condition (cf. (6.14))

$$\varphi' = \bar{\varphi}', \tag{8.3}$$

the current-continuity condition (cf. (7.5) and (7.22))

$$\frac{\partial \varphi'}{\partial r} = R \frac{\partial \bar{\varphi}'}{\partial r}, \tag{8.4}$$

and the far-field condition (cf. (5.18*a*))

$$\varphi' \sim -r \cos\theta. \tag{8.5}$$

The solenoidal velocity fields $\boldsymbol{u}' = \hat{\boldsymbol{e}}_r u' + \hat{\boldsymbol{e}}_\theta v'$ and $\bar{\boldsymbol{u}}' = \hat{\boldsymbol{e}}_r u' + \hat{\boldsymbol{e}}_\theta v'$ satisfy the homogeneous Stokes equations (cf. (5.16))

$$\boldsymbol{\nabla} p' = \nabla^2 \boldsymbol{u}', \quad M \boldsymbol{\nabla} \bar{p}' = \nabla^2 \bar{\boldsymbol{u}}', \tag{8.6a,b}$$

the impermeability condition (cf. (6.18))

$$u' = \bar{u}' = 0, \tag{8.7}$$

tangential-velocity continuity (cf. (6.17))

$$v' = \bar{v}', \tag{8.8}$$

shear-stress continuity (see (7.19))

$$\frac{\partial v'}{\partial r} - v' - M^{-1} \left(\frac{\partial \bar{v}'}{\partial r} - \bar{v}' \right) = \Lambda' \frac{\partial \varphi'}{\partial \theta}, \tag{8.9}$$

and far-field attenuation (cf. (7.23))

$$\boldsymbol{u}' \to \boldsymbol{0}. \tag{8.10}$$

The apparent surface-charge density Λ' appearing in (8.9) is provided by the effective Gauss condition (cf. (7.11))

$$\Lambda' = \frac{\partial \varphi'}{\partial r} - S^{-1} \frac{\partial \bar{\varphi}'}{\partial r}. \tag{8.11}$$

Finally, the conductivity ratio R appearing in (8.4) is provided by (cf. (6.30) and (7.22))

$$R = M \sqrt{\frac{K^+ K^-}{\bar{K}^+ \bar{K}^-}}. \tag{8.12}$$

https://doi.org/10.1017/jfm.2015.242 Published online by Cambridge University Press

The derived macroscale model thus differs from the Taylor–Melcher model in that surface-charge convection is absent in (8.4). It accordingly coincides with the model solved by Taylor (1966) in his pioneering analysis, where charge convection was neglected as a mere convenience. In the absence of that nonlinear mechanism, the electrostatic problem is linear and uncoupled to the flow; it can thus be solved independently. With the electric field (and the surface-charge density) known, the linear flow problem is readily solved. The resulting quadrupolar flow structure, provided in Melcher & Taylor (1969), confirms *a posteriori* the assumption made in § 5 of an open-streamlines topology.

As shown in § 7.6, the normal-stress jump evaluated based upon the macroscale model coincides with the true jump, as predicted by the microscale variables. The above macroscale description may accordingly be utilized to evaluate drops deformation at small capillary numbers. Given (4.35), the $O(\beta^2)$ normal-stress jump in the electrokinetic normalization (where stresses are scaled by $\epsilon_* \varphi_*^2/a_*^2$) corresponds to a jump of order $\epsilon_* \mathscr{E}_*^2$: the familiar leaky dielectric stress scale. Using that scale, the normal-stress jump is provided by (cf. (B 13))

$$-p' + \bar{p}' + 2\left(\frac{\partial u'}{\partial r} - M^{-1}\frac{\partial \bar{u}'}{\partial r}\right) + \frac{1}{2}\left[\left(\frac{\partial \varphi'}{\partial r}\right)^2 - S^{-1}\left(\frac{\partial \bar{\varphi}'}{\partial r}\right)^2\right] - \frac{1}{2}(1 - S^{-1})\left(\frac{\partial \varphi'}{\partial \theta}\right)^2. \tag{8.13}$$

Given its coincidence with the Taylor–Melcher description, our macroscale model would predict the same deformation from a spherical shape as that calculated by Torza *et al.* (1971).

9. Comparison with Baygents & Saville (1989)

9.1. *Direct inner–outer matching?*

As already mentioned, the microscale model employed herein is essentially that used by Baygents & Saville (1989). The only simplification here is the focus upon binary electrolyte solutions, as opposed to the more general case of N ionic species considered by Baygents & Saville (1989). The limit process (5.1) and (5.2) used to derive the macroscale model is also adopted from Baygents & Saville (1989). In contrast to our successful matching procedure, however, Baygents & Saville (1989) found it impossible to directly match the inner (Debye layer) and outer (bulk) regions. In what follows we discuss the difference between their analysis and ours.

In the course of their matching procedure, Baygents & Saville (1989) obtained N equations relating the dimensionless dipole strength of the drop to the $2N$ ionic mobilities (inside and outside the drop) and $2N$ ionic 'bulk' concentrations. They then explain that these equations over-specify the dipole strength 'since the ionic mobilities and bulk concentrations are fixed quantities': see equation (4.2), etc., in Baygents & Saville (1989). Given this over-specification, Baygents & Saville (1989) concluded that the inner and outer regions cannot be matched directly and resorted to a separate analysis of an intermediate boundary layer, of thickness $1/\beta$, where 'all three transport modes (convection, diffusion and electromigration) are important'. That layer resembles the diffusive boundary layer appearing in forced-convection heat- and mass-transfer problems (Acrivos & Goddard 1965). The details of that intermediate-layer analysis and its matching with the inner and outer regions are not provided by Baygents & Saville (1989); they nonetheless assert that these procedures eventually results in the familiar quadrupolar flow of Taylor (1966).

https://doi.org/10.1017/jfm.2015.242 Published online by Cambridge University Press

It appears that Baygents & Saville (1989) have overlooked the Einstein–Smoluchowski relation, which implies that the ratio of the ionic conductivities in the respective phases is independent of the specific species k ($1 \leqslant k \leqslant N$) considered. This is clearly illustrated in the binary case ($N = 2$) addressed in the present paper, where it is readily verified that the two equations governing the dipole strength simply coincide, giving its value (in the present notation) as $(M\bar{c}_0 - 1)/(M\bar{c}_0 + 2)$. Moreover, since $M\bar{c}_0$ coincides with the conductivity ratio R (see (7.22)), this dipole strength turns out identical to that which would be obtained from the electrohydrodynamic model (8.2)–(8.11): see indeed e.g. equation (25) in Melcher & Taylor (1969). It thus seems that the general approach of Baygents & Saville (1989), allowing for arbitrary number N of ionic species, tends to obscure the above-mentioned simplifying points. Indeed, for $N > 2$ the 'bulk' concentrations are not necessarily identical, significantly complicating the interpretation of equation (4.2) in Baygents & Saville (1989). It is unclear whether the simplifying arguments we have employed may be extended to the general problem of $N > 2$.

9.2. *Diffusive boundary layer*

Does the present analysis also give rise to the emergence of a diffusive boundary layer? The $O(\beta^2)$ ionic convection across the $O(\delta)$-wide Debye layer results in an $O(\delta\beta^2)$ 'surface current' of salt. As this current is generally nonuniform, ionic conservation implies that a comparable flux must be supplied from and into the electro-neutral bulk. It may appear as though this salt flux would give rise to $O(\delta\beta^2)$ salt gradients in the bulk; these, however, are incompatible with (5.13). A diffusive boundary is thus formed, where diffusion is balanced by advection; its thickness is accordingly $1/\beta$. (By (5.2), this narrow layer is much thicker than the Debye layer.) To accommodate the salt fluxes emerging from the Debye layer, the ratio of the excess-salt concentration in that layer to its $O(1/\beta)$ thickness must be $O(\delta\beta^2)$: that excess concentration thus turns out $O(\delta\beta)$, and is accordingly asymptotically small.

We have encountered similar incompatibilities in various electrokinetic problems (Yariv, Schnitzer & Frankel 2011; Schnitzer & Yariv 2012*b*; Schnitzer *et al.* 2013), where they are also resolved by the introduction of an intermediate diffusion layer. In these problems, the presence of the diffusive layer had no effect on the leading-order inner and outer solutions, hence its resolution was not required for a successful leading-order asymptotic matching between them. The situation in the present problem is similar. The structure of the diffusive boundary layer is thus tacitly ignored in the preceding analysis.

10. Concluding remarks

Starting from a 'first-principles' electrokinetic description of a drop exposed to an externally imposed electric field, we have derived a macroscale description valid in the double limit of thin Debye layers and strong applied field. This limit, first identified by Baygents & Saville (1989), represents electrohydrodynamic flows of leaky dielectric liquids. Our description nearly coincides with the Taylor–Melcher model; moreover, the drop deformation may also be calculated using the stresses predicted by the macroscale model. On the other hand, our analysis reveals that charge convection, explicit in the general description of Melcher & Taylor (1969), does not enter the macroscale description. Another difference with the scheme of Melcher & Taylor (1969) has to do with the conductivity ratio. While in Melcher & Taylor (1969) this ratio is considered as a specified parameter, representing liquid

https://doi.org/10.1017/jfm.2015.242 Published online by Cambridge University Press

properties, our analysis reveals that the 'conductivity' of the drop phase depends upon the adsorption kinetics at the interface, and is accordingly a function of the liquid–liquid system considered. Finally, our analysis elucidates the role played by the non-zero net charge of the drop and the accompanying diffuse-charge layer. These new insights into the fundamentals of electrohydrodynamics may be useful in studying phenomena in which the validity of the leaky-dielectric model is dubious, such as vesicles (Salipante & Vlahovska 2014) and electrowetting with electrolytes (Monroe *et al.* 2006), or systems in which both electrokinetic and electrohydrodynamic effects are important (Schnitzer *et al.* 2014).

In what follows we address these issues in detail, and discuss the relation between our unified approach and the problem of drop electrophoresis in the thin Debye-layer limit.

10.1. *The Baygents–Saville limit*

In deriving the macroscale model for the electrokinetic transport we have employed the Baygents–Saville limit (5.1) and (5.2). Following this derivation, the necessities for imposing the restrictions specifying this limit process become evident. The assumption $\beta \gg 1$ results in uniform salt concentrations in both the suspending liquid and the drop phase. It also results in the domination of the fore–aft symmetric $O(\beta^2)$ electrohydrodynamic flow pattern over the $O(\beta)$ electro-osmotic flow animating the drop phoretic motion. The restriction (5.2) is also necessary for the self-consistency of our asymptotic expansions: when β scales as $1/\delta$, tangential ionic advection with the Debye layer become $O(\delta^{-2})$ large, thus necessitating a transversely varying $O(\delta^{-1})$ normal fluxes. The Debye layer is not at quasi-equilibrium, and the entire scheme collapses.

The limitations imposed by the Baygents–Saville limit are naturally met in leaky dielectric electrohydrodynamic phenomena. As drops are typically much larger than colloidal particles, equation (5.1) is easily satisfied for virtually all practical values of the salt concentration $\mathscr{C}_*$: see definitions (4.6) and (4.35). Incidentally, these definitions also imply that the product $\delta\beta$ is independent of the drop size a_*: satisfaction of (5.2) thus essentially limits the magnitude of the applied field $\mathscr{E}_*$, or, more precisely, of $\mathscr{E}_*^2/\mathscr{C}_*$.

Note that, at least until recently (Schnitzer *et al.* 2013; Schnitzer & Yariv 2013; Schnitzer *et al.* 2014), virtually all electrokinetic analyses of drops under electric fields had actually addressed the limit of weak applied fields, see e.g. Ohshima *et al.* (1984) and Baygents & Saville (1991).

10.2. *Absence of surface-charge convection*

The linearity of the electrostatic problem, which enables analytic solution of the macroscale model, follows from the absence of surface convection of charge. In our macroscale model, this absence automatically follows from the Baygents–Saville limit (1.1). Indeed, for the effective $O(\delta\beta^2)$ surface current associated with the leading $O(\beta^2)$ flow to enter the ion conservation equation (4.26) at the $O(\beta)$ leading order, β must be $O(\delta^{-1})$. Such large values of the applied field do not satisfy the restriction (5.2).

In fact, the surface current associated with the leading $O(\beta^2)$ flow is even smaller than $O(\delta\beta^2)$. Indeed, as the $O(\beta^2)$ tangential velocity is transversely uniform (see (6.16)), the $O(\delta\beta^2)$ surface current is simply provided by its product with the apparent $O(1)$ Debye-layer charge; the latter, however, vanishes by screening (see (6.32)). It

https://doi.org/10.1017/jfm.2015.242 Published online by Cambridge University Press

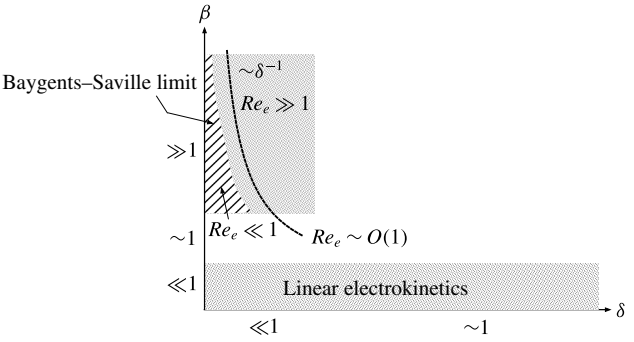


FIGURE 2. The Taylor–Melcher leaky dielectric essentially constitutes a coarse-grained electrokinetic model in the Baygents–Saville limit of strong fields $\beta \gg 1$ and thin Debye layers, $\delta \ll 1$, with $1 \ll \beta \ll \delta^{-1}$. This limit corresponds to small electric Reynolds numbers, $Re_e \ll 1$, which is consistent with the absence of surface-charge advection in the derived macroscale model.

may therefore appear that the leading-order surface current is due to the leading $O(\delta\beta)$ apparent charge, and is accordingly $O(\delta^2\beta^3)$. Note however that another source for a surface current is the $O(\beta)$ electro-osmotic flow, which we did not bother to calculate. As this flow is transversely non-uniform, it results through advection of the $O(1)$ ionic densities in an $O(\delta\beta)$ surface current. The Baygents–Saville restriction (5.2) does not determine which of these two effects dominates. The corrections implied by these currents to the charge-conservation condition (7.5), where the Ohmic currents are $O(\beta)$, are of relative orders $(\delta\beta)^2$ and δ, respectively.

In the electrohydrodynamic literature, the neglect of charge convection is conventionally associated with the assumption of small electric Reynolds number (see Melcher & Taylor 1969). Consider indeed the typical dimensional magnitude of the respective charge conduction and convection terms in a surface-charge balance (e.g. equation (Il) in Melcher & Taylor 1969). The former is of order $\sigma_*\mathscr{E}_*$, σ_* being a typical conductivity, while the latter, represented by a surface-divergence term, is of order $\Lambda_* v_*/a_*$, where Λ_* is the apparent surface-charge density; in the leaky dielectric description, that density is of order $\epsilon_*\mathscr{E}_*$. It follows that the ratio of charge convection to conduction is of order $\epsilon_* v_*/\sigma_* a_*$. This is the electric Reynolds number Re_e.

Following our derivation of the electrohydrodynamic Taylor–Melcher model as a coarse-grained description, this number is easily estimated. Consider the simple case of equal diffusivities $D_*^{\pm} = D_*$, where $\alpha^{\pm}$ are identical, $=\alpha$ say (see (4.4)). The bulk conductivity σ_* is then given by $2ze_*\mathscr{C}_* D_*/\varphi_*$, see (7.21). Using the leaky dielectric velocity scale $\epsilon_* a_* \mathscr{E}_*^2/\mu_*$ we readily find using definitions (4.1), (4.4), (4.6) and (4.35) that

$$Re_e = \alpha\delta^2\beta^2. \tag{10.1}$$

Since α is typically $O(1)$ (see (4.4) etc.), the electric Reynolds number is asymptotically small in the Baygents–Saville limit (1.1) underlying our electrokinetic description: see figure 2.

In the classical paper of Melcher & Taylor (1969), charge convection is presented in the electrohydrodynamic model (see their Table I). It is then neglected throughout when performing steady analyses of specific configurations: in particular, in the analysis of the flow about a leaky dielectric drop. This neglect is introduced as an

https://doi.org/10.1017/jfm.2015.242 Published online by Cambridge University Press

additional assumption. As Melcher & Taylor (1969) had no underlying electrokinetic model to provide the magnitude of the bulk conductivity, they could not have obtained the estimate (10.1).

Note that the parts of the analysis of Melcher & Taylor (1969) which deal with instabilities and fluid motion driven by alternating currents allow for finite electric Reynolds number. Moreover, charge convection was incorporated in several electrohydrodynamic models (see Feng & Scott 1996; Xu & Homsy 2006; Salipante & Vlahovska 2010) in an attempt to improve upon Taylor's initial analysis. In view of estimate (10.1), these studies fall outside the Baygents and Saville regime, and hence their electrokinetic interpretation remains unclear.

10.3. *The conductivity ratio: a material property?*

The macroscale equations depend upon the permittivity ratio S, the viscosity ratio M and the conductivity ratio R, just as in the model outlined by Melcher & Taylor (1969). Melcher & Taylor (1969) consider these parameters as given material ratios. In our scheme there is however a conceptual difference between the permittivity and viscosity ratios S and M and the conductivity ratio R: while the former two indeed represent (ratios between) true material properties (and actually appear in the microscope formulation), the latter is a derived macroscale quantity, which does not appear in the original formulation. In view of expression (8.12), moreover, R depends upon the adsorption coefficients $(K^{\pm}, \bar{K}^{\pm})$ (normalized by $2/\kappa_*$), and accordingly cannot be considered a material property. Putting it differently, while the conductivity of the suspending liquid can be conceptually measured in an experiment, independently of the drop, the same does not hold for the drop conductivity.

This difference with the Taylor–Melcher model should be viewed with caution, however, given our simplistic modelling of charge transfer across the interface and our simplifying assumption of a strong binary electrolyte. A more realistic description of ionic transport would incorporate bulk reactions (see e.g. Saville 1997) and allow only several of the ionic species to pass through the interface. Within the framework of such a general model, one can envisage two scenarios where the drop-phase conductivity is effectively a property of the drop, unaffected by the passage of currents. The first is realized in the limit of fast reactions, while the second occurs when the ionic composition in the two liquids consists of a high concentration of 'inert' salt ions (for which the adsorption coefficients vanish), which essentially determines the bulk conductivity, and a small concentration of ions which undergo interfacial sorption, thereby enabling the passage of electric current through the interface.

10.4. *Highly conducting drops*

A familiar feature of the flow field predicted by the leaky-dielectric model is that it vanishes in the limit $R \gg 1$. This implies that, for sufficiently large R, the (formally subdominant) electrokinetic flow associated with the presence of equilibrium charge becomes comparable with the (formally dominant) leaky-dielectric flow. The field strengths at which this transition occurs, and hence at which the leaky-dielectric cannot be expected to apply, can be easily estimated from our analysis. On the one hand, inspection of the macroscale equations of § 8 reveals that the Taylor–Melcher flow vanishes like $1/R$ as $R \to \infty$; this corresponds to an $O(\beta^2/R)$ flow in terms of the electrokinetic scalings of § 4. On the other hand, our analysis reveals that the electrokinetic velocity is $O(\beta)$, and does not vanish with R. Thus, the derived macroscale model collapses when $R \sim O(\beta)$.

https://doi.org/10.1017/jfm.2015.242 Published online by Cambridge University Press

10.5. *Net drop charge and electrophoresis*

We now discuss the net drop charge: namely the total charge held by the interface in the absence of external field. In the Taylor–Melcher description, the dipolar charge distribution clearly implies that such a net charge is absent. Moreover, no diffuse layer accompanies, either explicitly or implicitly, the local interfacial charge. Indeed, in the introduction to his review paper, Saville (1997) wrote that 'With ... leaky dielectrics, diffuse layers associated with equilibrium charge are usually absent'. This claim is refuted here: our electrokinetic analysis naturally allows the presence of equilibrium charge at the interface, which is screened by diffuse-charge layers. The amount of equilibrium charge is simply set by the interfacial kinetics, and would vanish only for specifically chosen combinations of the respective coefficients. In the physicochemical model (4.32), zero drop charge is realized for $K^+ = K^- = \bar{K}^+ = \bar{K}^-$ and $S = 1$: see (6.27) and (6.29). In the general case, then, the charge on the genuine interface is non-zero. In fact, the presence of non-zero interfacial charge is actually necessary for the validity of our asymptotic scheme, which hinges upon the induced charge being a small perturbation.

Our analysis reveals that, remarkably, the electrophoretic motion engendered by the net drop charge constitutes an asymptotic correction to the Taylor–Melcher flow, itself animated by a perturbation to that equilibrium charge. The appearance of electrophoresis at a higher order might be consistent with existing experiments, where the drop indeed tends to move under the electric field. (Such motion was considered as an inevitable inconvenience that interferes with the convenient observation and measurement of electrohydrodynamic drop deformation, see Taylor (1966) and Vizika & Saville (1992).)

Our unified approach provides the means for understating this inevitable motion, which apparently goes hand in hand with the Taylor–Melcher flow. The calculation of drop electrophoresis in our scheme requires continuing the asymptotic analysis towards deriving a higher-order macroscale model. Such an analysis reveals that drop electrophoresis is animated by both shear and a two-sided electro-osmotic slip mechanism. While the latter is already implied in our analysis (see (7.13)), the calculation of the shear contribution entails a complicated calculation, including the resolution of the two diffusive boundary layers. In the limit of a highly viscous drop, one can show that the shear contribution becomes trivial. The drop thus migrates according to a Smoluchowski-type formula, with the zeta potential appearing therein being that of the external Debye layer. Interestingly then, the equilibrium charge in that case cannot be straightforwardly inferred from electrophoretic measurements.

The compatibility of non-zero net charge with the absence of electrophoresis at leading order is clearly a manifestation of the delicate limit process (1.1), representing the strong fields characterizing Taylor–Melcher flows. This compatibility casts doubts regarding the applicability of the scheme developed by Zholkovskij, Masliyah & Czarnecki (2002). In that paper, which proposes a different approach to model the transition from electrokinetics to electrohydrodynamics, the Taylor–Melcher description is developed for an arbitrary Debye length. In sharp contrast to Baygents & Saville (1989), this is accomplished via a weak-field approximation. Putting aside the validity of such an approximation in describing Taylor–Melcher flows, it appears that the main shortcoming in the analysis of Zholkovskij *et al.* (2002) is the necessity of assuming zero net charge; as the authors explain, this corresponds to artificially specifying appropriate ratios of the kinetic parameters. Similarly, the recent stability analysis of Gambhire & Thaokar (2014) also makes use of an effective weak-field linearization. In that paper the authors avoid the arbitrariness in the kinetic approach

https://doi.org/10.1017/jfm.2015.242 Published online by Cambridge University Press

of Zholkovskij *et al.* (2002) by focusing upon inert solute which does not adsorb to the genuine interface. While this gives rise to a consistent physical model, the absence of ionic transport through the interface renders it insufficient when attempting to describe the electrokinetics underlying the leaky-dielectric model.

Acknowledgement

This research was supported by the Israel Science Foundation (grant number 184/12).

Appendix A. Salt uniformity

Since the flow fields $\boldsymbol{u}_{-2}$ and $\bar{\boldsymbol{u}}_{-2}$ are steady in the comoving reference frame we employ, (5.11) state that c_0 and $\bar{c}_0$ are constant along the respective streamlines of these fields. For open streamlines which originate at infinity such constancy would readily provide the values of c_0 using its far-field distribution (given here by (4.33*a*)), thus leading to the uniform salt distribution (5.12). We now show that $\bar{c}_0$ is uniform as well. We follow a method devised by Batchelor (1956) in the different context of vorticity dynamics at large-Reynolds-number flow.

The proof makes use of (i) the fact that the streamlines of the steady flow $\bar{\boldsymbol{u}}_{-2}$ are bounded by the drop boundary and are accordingly all closed; and (ii) the axial symmetry of the leading-order flow. We employ the integral form of the salt balance (4.21),

$$\oint_{\mathscr{S}} \mathrm{d}A\, \hat{\boldsymbol{n}} \cdot \left\{ \bar{\boldsymbol{j}} + \left(\frac{\alpha^+ + \alpha^-}{2} \bar{c} + \frac{\alpha^+ - \alpha^-}{2} \bar{q} \right) \bar{\boldsymbol{u}} \right\} = 0, \tag{A 1}$$

wherein $\mathscr{S}$ is the boundary of an arbitrary domain lying entirely within the drop phase and $\hat{\boldsymbol{n}}$ is a unit vector normal to $\mathscr{S}$. Specifically, consider a streamline of $\bar{\boldsymbol{u}}$ and imagine the torus-like surface $\mathscr{S}$ formed by rotating it about the symmetry axis. As $\hat{\boldsymbol{n}} \cdot \bar{\boldsymbol{u}} = 0$ on that surface, equation (A 1) reads

$$\oint_{\mathscr{S}} \mathrm{d}A\, \hat{\boldsymbol{n}} \cdot \bar{\boldsymbol{j}} = 0. \tag{A 2}$$

We now consider the limit $\delta \to 0$, where $\bar{\boldsymbol{u}} \to \bar{\boldsymbol{u}}_{-2}$. Because of axial symmetry, $\bar{\boldsymbol{u}}_{-2}$ is derived from a Stokes streamfunction, say $\bar{\psi}_{-2}$. Since $\bar{c}_0$ is constant on the streamlines of $\bar{\boldsymbol{u}}_{-2}$, it follows that it is a function of $\bar{\psi}_{-2}$. As $\delta \to 0$, then, $\mathscr{S}$ is given by a constant-ψ_{-2} surface, while $\bar{\boldsymbol{j}} \to \bar{\boldsymbol{j}}_0$:

$$\oint_{\bar{\psi}_{-2}=\text{const.}} \mathrm{d}A\, \hat{\boldsymbol{n}} \cdot \bar{\boldsymbol{j}}_0 = 0. \tag{A 3}$$

Use of (5.8*b*) then yields

$$\oint_{\bar{\psi}_{-2}=\text{const.}} \mathrm{d}A\, \frac{\partial \bar{c}_0}{\partial n} = 0. \tag{A 4}$$

At this point we conceptually construct a system of (ξ, η) orthogonal coordinates in the meridian plain with $\xi = \bar{\psi}_{-2}$ and the level curves of η orthogonal to those of $\bar{\psi}_{-2}$. The fluid domain is therefore described via a curvilinear (ξ, η, ϖ) coordinate system, ϖ being the azimuthal angle already defined in § 4.3. In these coordinates,

https://doi.org/10.1017/jfm.2015.242 Published online by Cambridge University Press

$\bar{c}_0$ is a function of ξ alone, independent of η and ϖ. Moreover, since the integration domain in (4.3) is a consent-ξ surface, it is evident (tacitly choosing $\hat{\boldsymbol{n}}$ pointing in the direction of increasing $\bar{\psi}_{-2}$) that on that surface $\partial\bar{c}_0/\partial n = (1/h_\xi)\mathrm{d}\bar{c}_0/\mathrm{d}\xi$, where h_ξ is the metric coefficient associated with the curvilinear coordinate ξ (in general, a function of both ξ and η). As $\mathrm{d}\bar{c}_0/\mathrm{d}\xi$, a function of ξ, is constant on the integration surface, it may be taken outside the integral. Equation (A 4) becomes

$$\frac{\mathrm{d}\bar{c}_0}{\mathrm{d}\xi}\oint_{\xi=\text{const.}}\frac{\mathrm{d}A}{h_\xi}=0. \tag{A 5}$$

Since $h_\xi > 0$, this implies that

$$\frac{\mathrm{d}\bar{c}_0}{\mathrm{d}\xi}=0. \tag{A 6}$$

Since the integration domain is an arbitrary stream surface, equation (A 6) holds for all values of $\xi(=\bar{\psi}_{-2})$. It follows that $\bar{c}_0$ is independent of $\bar{\psi}_{-2}$ and hence uniform.

Appendix B. Normal-stress jump

Expressed in terms of the Debye-layer variables, the microscale normal-stress jump across the interface is provided by the expression:

$$-P-\bar{P}+2\left(\frac{\partial U}{\partial Z}-M^{-1}\frac{\partial\bar{U}}{\partial Z}\right)\delta^{-1}+\frac{1}{2\delta^2}\left[\left(\frac{\partial\Phi}{\partial Z}\right)^2-S^{-1}\left(\frac{\partial\bar{\Phi}}{\partial Z}\right)^2\right]-\frac{1}{2}(1-S^{-1})\left(\frac{\partial\Phi}{\partial\theta}\right)^2. \tag{B 1}$$

In what follows we express this quantity in terms of the macroscale variables.

Inspection of the radial momentum balance in the Debye layer suggests the pressure expansion

$$P=\delta^{-2}P_{-2,0}+\delta^{-1}\beta P_{-1,-1}+\delta^{-1}P_{-1,0}+\beta^2P_{0,-2}+\cdots. \tag{B 2}$$

The radial momentum balance at leading $O(\delta^{-3})$ reads

$$\frac{\partial P_{-2,0}}{\partial Z}=\frac{\partial^2\Phi_{0,0}}{\partial Z^2}\frac{\partial\Phi_{0,0}}{\partial Z}. \tag{B 3}$$

Since the bulk pressure is only $O(\beta^2)$, and given the exponential decay of $\Phi_{0,0}$ as $Z\to\infty$, integration of (B 3) simply yields

$$P_{-2,0}=\frac{1}{2}\left(\frac{\partial\Phi_{0,0}}{\partial Z}\right)^2. \tag{B 4}$$

A similar expression is obtained for $\bar{P}_{-2,0}$:

$$\bar{P}_{-2,0}=\frac{1}{2S}\left(\frac{\partial\bar{\Phi}_{0,0}}{\partial Z}\right)^2. \tag{B 5}$$

Substitution into (B 1) thus reveals that the stress jump at $O(\delta^{-2})$ trivially vanishes.

Continuing on, the radial momentum balance at $O(\delta^{-2}\beta)$ reads

$$\frac{\partial P_{-1,-1}}{\partial Z}=\frac{\partial^2\Phi_{0,0}}{\partial Z^2}\frac{\partial\Phi_{1,-1}}{\partial Z}+\frac{\partial^2\Phi_{1,-1}}{\partial Z^2}\frac{\partial\Phi_{0,0}}{\partial Z}. \tag{B 6}$$

https://doi.org/10.1017/jfm.2015.242 Published online by Cambridge University Press

Noting again the rapid decay of $\Phi_{0,0}$ and the absence of $O(\delta^{-1}\beta)$ bulk pressure, we obtain

$$P_{-1,-1} = \frac{\partial \Phi_{0,0}}{\partial Z}\frac{\partial \Phi_{1,-1}}{\partial Z}, \tag{B 7}$$

with a similar expression in the drop phase,

$$\bar{P}_{-1,-1} = S^{-1}\frac{\partial \bar{\Phi}_{0,0}}{\partial Z}\frac{\partial \bar{\Phi}_{1,-1}}{\partial Z}. \tag{B 8}$$

Substitution into (B 1) reveals that the stress jump at $O(\delta^{-1}\beta)$ vanishes as well.

Returning to the radial momentum balance, this time at $O(\delta^{-2})$, we find

$$\frac{\partial P_{-1,0}}{\partial Z} = 2\left(\frac{\partial \Phi_{0,0}}{\partial Z}\right)^2, \tag{B 9}$$

representing the effect of drop curvature. Integrating with respect to Z from 0 to ∞, where $P_{-1,0}$ must vanish due to the absence of $O(\delta^{-1})$ pressure term in the bulk, we find that $P_{-1,0}(Z=0)$ is provided by a quadrature of $\partial\Phi_{0,0}/\partial Z$. Since this derivative is independent of θ (see § 6.3), so must be $P_{-1,0}(Z=0)$. A similar argument applies for $\bar{P}_{-1,0}(Z=0)$. Since a uniform normal-stress jump does not contribute to a deformation from sphericity, it may be disregarded.

Finally, the radial momentum balance at $O(\delta^{-1}\beta^2)$ reads

$$\frac{\partial P_{0,-2}}{\partial Z} = \frac{\partial^2 U_{1,-2}}{\partial Z^2} + \frac{\partial^2 \Phi_{1,-1}}{\partial Z^2}\frac{\partial \Phi_{1,-1}}{\partial Z}. \tag{B 10}$$

Integrating, and using the matching conditions

$$P_{0,-2} \to p_{0,-2}, \quad \frac{\partial U_{1,-2}}{\partial Z} \to \frac{\partial u_{0,-2}}{\partial r}, \quad \frac{\partial \Phi_{1,-1}}{\partial Z} \to \frac{\partial \varphi_{0,-1}}{\partial r}, \tag{B 11a–c}$$

we find that

$$P_{0,-2} - \frac{\partial U_{1,-2}}{\partial Z} = p_{0,-2} - \frac{\partial u_{0,-2}}{\partial r} - \frac{1}{2}\left(\frac{\partial \varphi_{0,-1}}{\partial r}\right)^2 + \frac{1}{2}\left(\frac{\partial \Phi_{1,-1}}{\partial Z}\right)^2. \tag{B 12}$$

Repeating the calculation for the drop-phase pressure at this order, we find that the first non-vanishing (and non-constant) normal-pressure jump is $O(\beta^2)$, namely

$$\beta^2\left\{-p_{0,-2} + \bar{p}_{0,-2} + 2\left(\frac{\partial u_{0,-2}}{\partial r} - M^{-1}\frac{\partial \bar{u}_{0,-2}}{\partial r}\right)\right.$$
$$\left. + \frac{1}{2}\left[\left(\frac{\partial \varphi_{0,-1}}{\partial r}\right)^2 - S^{-1}\left(\frac{\partial \bar{\varphi}_{0,-1}}{\partial r}\right)^2\right] - \frac{1}{2}\left(1 - S^{-1}\right)\left(\frac{\partial \varphi_{0,-1}}{\partial \theta}\right)^2\right\}. \tag{B 13}$$

This however is the expression which would be provided using the effective macroscale model.

https://doi.org/10.1017/jfm.2015.242 Published online by Cambridge University Press

REFERENCES

ACRIVOS, A. & GODDARD, J. D. 1965 Asymptotic expansions for laminar forced-convection heat and mass transfer. Part 1. Low speed flows. *J. Fluid Mech.* **23** (02), 273–291.

ANDERSON, J. L. 1989 Colloid transport by interfacial forces. *Annu. Rev. Fluid Mech.* **30**, 139–165.

BATCHELOR, G. 1956 On steady laminar flow with closed streamlines at large Reynolds number. *J. Fluid Mech.* **1** (2), 177–190.

BAYGENTS, J. C. & SAVILLE, D. A. 1989 The circulation produced in a drop by an electric field: a high field strength electrokinetic model. In *Drops & Bubbles, Third International Colloquium, Monterey 1988* (ed. T. Wang), AIP Conference Proceedings, vol. 7, pp. 7–17. American Institute of Physics.

BAYGENTS, J. C. & SAVILLE, D. A. 1991 Electrophoresis of drops and bubbles. *J. Chem. Soc. Faraday Trans.* **87** (12), 1883–1898.

BEN, Y., DEMEKHIN, E. A. & CHANG, H.-C. 2004 Nonlinear electrokinetics and 'superfast' electrophoresis. *J. Colloid Interface Sci.* **276**, 483–497.

CHU, K. T. & BAZANT, M. Z. 2006 Nonlinear electrochemical relaxation around conductors. *Phys. Rev.* E **74** (1), 011501.

CRASTER, R. V. & MATAR, O. K. 2005 Electrically induced pattern formation in thin leaky dielectric films. *Phys. Fluids* **17** (3), 032104.

DERJAGUIN, B. V. & DUKHIN, S. S. 1974 Nonequilibrium double layer and electrokinetic phenomena. In *Electrokinetic Phenomena* (ed. E. Matijevic), Surface and Colloid Science, vol. 7, pp. 273–336. John Wiley & Sons.

FENG, J. Q. 1999 Electrohydrodynamic behaviour of a drop subjected to a steady uniform electric field at finite electric Reynolds number. *Proc. R. Soc. Lond.* A **455** (1986), 2245–2269.

FENG, J. Q. & SCOTT, T. C. 1996 A computational analysis of electrohydrodynamics of a leaky dielectric drop in an electric field. *J. Fluid Mech.* **311**, 289–326.

GAMBHIRE, P. & THAOKAR, R. 2014 Electrokinetic model for electric-field-induced interfacial instabilities. *Phys. Rev.* E **89** (3), 032409.

LEAL, L. G. 2007 *Advanced Transport Phenomena: Fluid Mechanics and Convective Transport Processes*. Cambridge University Press.

MANI, A. & BAZANT, M. Z. 2011 Deionization shocks in microstructures. *Phys. Rev.* E **84** (6), 061504.

MELCHER, J. R. & TAYLOR, G. I. 1969 Electrohydrodynamics: a review of the role of interfacial shear stresses. *Annu. Rev. Fluid Mech.* **1** (1), 111–146.

MONROE, C. W., DAIKHIN, L. I., URBAKH, M. & KORNYSHEV, A. A. 2006 Electrowetting with electrolytes. *Phys. Rev. Lett.* **97** (13), 136102.

MORRISON, F. A. 1970 Electrophoresis of a particle of arbitrary shape. *J. Colloid Interface Sci.* **34**, 210–214.

O'BRIEN, R. W. 1983 The solution of the electrokinetic equations for colloidal particles with thin double layers. *J. Colloid Interface Sci.* **92** (1), 204–216.

OHSHIMA, H., HEALY, T. W. & WHITE, L. R. 1984 Electrokinetic phenomena in a dilute suspension of charged mercury drops. *J. Chem. Soc. Faraday Trans.* **80** (12), 1643–1667.

RIVETTE, N. J. & BAYGENTS, J. C. 1996 A note on the electrostatic force and torque acting on an isolated body in an electric field. *Chem. Engng Sci.* **51** (23), 5205–5211.

SALIPANTE, P. F. & VLAHOVSKA, P. M. 2010 Electrohydrodynamics of drops in strong uniform dc electric fields. *Phys. Fluids* **22**, 112110.

SALIPANTE, P. F. & VLAHOVSKA, P. M. 2014 Vesicle deformation in DC electric pulses. *Soft Matt.* **10** (19), 3386–3393.

SAVILLE, D. A. 1977 Electrokinetic effects with small particles. *Annu. Rev. Fluid Mech.* **9**, 321–337.

SAVILLE, D. A. 1997 Electrohydrodynamics: the Taylor–Melcher leaky dielectric model. *Annu. Rev. Fluid Mech.* **29** (1), 27–64.

SCHNITZER, O., FRANKEL, I. & YARIV, E. 2013 Electrokinetic flows about conducting drops. *J. Fluid Mech.* **722**, 394–423.

SCHNITZER, O., FRANKEL, I. & YARIV, E. 2014 Electrophoresis of bubbles. *J. Fluid Mech.* **753**, 49–79.

https://doi.org/10.1017/jfm.2015.242 Published online by Cambridge University Press

SCHNITZER, O. & YARIV, E. 2012*a* Macroscale description of electrokinetic flows at large zeta potentials: nonlinear surface conduction. *Phys. Rev.* E **86**, 021503.

SCHNITZER, O. & YARIV, E. 2012*b* Strong-field electrophoresis. *J. Fluid Mech.* **701**, 333–351.

SCHNITZER, O. & YARIV, E. 2013 Nonlinear electrokinetic flow about a polarized conducting drop. *Phys. Rev.* E **87**, 041002R.

SCHNITZER, O., ZEYDE, R., YAVNEH, I. & YARIV, E. 2013 Nonlinear electrophoresis of a highly charged colloidal particle. *Phys. Fluids* **25**, 052004.

TAYLOR, G. 1966 Studies in electrohydrodynamics. I. The circulation produced in a drop by electrical field. *Proc. R. Soc. Lond.* A **291** (1425), 159–166.

TORZA, S., COX, R. G. & MASON, S. G. 1971 Electrohydrodynamic deformation and burst of liquid drop. *Phil. Trans. R. Soc. Lond.* A **269** (1198), 295–319.

VIZIKA, O. & SAVILLE, D. A. 1992 The electrohydrodynamic deformation of drops suspended in liquids in steady and oscillatory electric fields. *J. Fluid Mech.* **239** (1), 1–21.

XU, X. & HOMSY, G. M. 2006 The settling velocity and shape distortion of drops in a uniform electric field. *J. Fluid Mech.* **564**, 395–414.

YARIV, E. 2009 An asymptotic derivation of the thin-Debye-layer limit for electrokinetic phenomena. *Chem. Engng Commun.* **197**, 3–17.

YARIV, E. 2010 Migration of ion-exchange particles driven by a uniform electric field. *J. Fluid Mech.* **655**, 105–121.

YARIV, E., SCHNITZER, O. & FRANKEL, I. 2011 Streaming-potential phenomena in the thin-Debye-layer limit. Part 1. General theory. *J. Fluid Mech.* **685**, 306–334.

ZHOLKOVSKIJ, E. K., MASLIYAH, J. H. & CZARNECKI, J. 2002 An electrokinetic model of drop deformation in an electric field. *J. Fluid Mech.* **472** (1), 1–27.

https://doi.org/10.1017/jfm.2015.242 Published online by Cambridge University Press